UPTEC W11 015
Examensarbete 30 hp
Juni 2011

The significance of heterogeneity for spreading of geologically stored carbon dioxide

Betydelsen av heterogenitet för spridning av geologiskt lagrad koldioxid

---

Christofer Olofsson

ABSTRACT
The significance of heterogeneity for spreading of geologically stored carbon dioxide

Christofer Olofsson

The demand for large scale storage of carbon dioxide (CO_2) grows stronger as incentives to reduce greenhouse gas emissions are introduced. Geological storage sites such as depleted oil and gas reservoirs, unminable coal seams and deep saline water-saturated aquifers are a few of many possible geological storage sites. Geological formations offer large scale storage potential, hidden locations and are naturally occurring world wide. A disadvantage is the difficulty to investigate the properties of storage material over large areas.

Reservoir simulation studies addressing issues of heterogeneous reservoirs are growing in number. There is still much to investigate however this study adds to the field by investigating the significance of the heterogeneity in hydraulic conductivity based on core sample data. The data was received from the main CO_2 injection site Heletz, Israel in the European Union Seventh Framework Programme for research and technological development (EU FP7) project MUSTANG (CO_2MUSTANG, 2011-03-13). By developing models using iTOUGH2/ECO2N, the aim of this study is to contribute to a better understanding of how the *average permeability*, *variance in permeability* and *spatial correlation* of the reservoir properties affect the distribution of CO_2 within the deep saline aquifer target layer.

In this study a stochastic simulation approach known as the Monte Carlo method is applied. Based on core sample data, geostatistical properties of the data are determined and utilized to create equally probable realizations where properties are described through a probability distribution described by a mean and variance as well as a constructed semivariogram.

The results suggest that deep saline aquifers are less storage effective for higher values of average *permeability*, *variance in permeability* and *spatial correlation*. The results also indicate that the Heletz aquifer, with its highly heterogeneous characteristics, in some extreme cases can be just as storage effective as a deep saline aquifer ten times as permeable consisting of homogeneous sandstone.

Keywords: Storage efficiency, Heterogeneity, Variogram, iTOUGH2, ECO2N, Geological storage, CO_2, Saline aquifer.

Department of Earth Siences, Uppsala University, Villavägen 16, SE-752 36 Uppsala
ISSN 1401-5765

REFERAT
Betydelsen av heterogenitet för spridning av geologiskt lagrad koldioxid

Christofer Olofsson

Incitament för minskningar av växthusgaser har på senare tid ökat efterfrågan för storskalig lagring av koldioxid (CO_2). Geologiska lagringsplatser som exploaterade olje- och gasreservoarer, svårutvunna kollager och djupt belägna salina akvifärer är exempel på potentiella lagringsplatser. Sådana geologiska formationer erbjuder storskalig lagring, dold förvaring och är naturligt förekommande världen över. Dock finns det stora svårigheter i att undersöka de materiella egenskaperna för hela lagringsområden.

Simuleringsstudier som hantera frågor gällande reservoarers heterogenitet växer i antal. Det finns fortfarande mycket kvar att undersöka och denna studie bidrar till detta forskningsområde genom att undersöka betydelsen av heterogenitet i hydraulisk konduktivitet för spridningen av koldioxid med hjälp av uppmätt brunnsdata. Data erhölls från lagringsplatsen Heletz i Israel som är den huvudsakliga lagringplatsen i projektet MUSTANG är en del av den Europeiska Unionens sjunde ramprogram för forskning och teknisk utveckling (EU FP7), (CO2MUSTANG, 2011/3/13). Genom att utveckla modeller med hjälp av programvaran iTOUGH2/ECO2N är syftet med denna studie att bidra till en bättre förståelse för hur den genomsnittliga permeabilitet, varians i permeabilitet samt rumslig korrelation av reservoaregenskaper påverkar fördelningen av CO_2 i den djupa saltvattenakvifären Heletz.

Denna studie använde sig av stokastisk simulering genom att tillämpa Monte Carlo-metoden. Med hjälp av tidigare uppmätt brunnsdata kunde geostatistiska egenskaper bestämmas för att skapa ekvivalent sannolika realiseringar. De geostatistiska egenskaperna beskrevs med en sannolikhetsfördelning genom medelvärde och varians samt ett konstruerat semivariogram.

Resultaten tyder på att djupa saltvattenakvifärer är mindre lagringseffektiva vid högre värden av genomsnittlig permeabilitet, varians i permeabilitet och rumslig horisontell korrelation. Resultaten visar även att Heletz akvifär, med dess mycket heterogena egenskaper, i extrema fall kan vara lika lagringsineffektiv som en djupt belägen saltvattenakvifär med tio gånger högre genomsnittlig permeabilitet.

Nyckelord: Lagringseffektivitet, Heterogenitet, Variogram, iTOUGH2, ECO2N, Geologisk lagring, CO_2, Saltvattenakvifär.

Institutionen för Geovetenskaper, Uppsala Universitet, Villavägen 16, SE-752 36 Uppsala
ISSN 1401-5765

PREFACE

This master thesis is the final stage in the Civil Engineering program *Aquatic and Environmental Engineering* at Uppsala University, Sweden. The thesis is equivalent to 30 Swedish university credits and has been done for the department of Earth Sciences, Air, Water and Landscape Sciences, Uppsala University with supervision from Assistant Professor Fritjof Fagerlund. Subject reviewer for this thesis is Professor Auli Niemi.

I wish to thank Fritjof Fagerlund for his grand support, expertise and motivation given despite his many other assignments, projects and busy schedule. I also wish to thank Liang Tian for contributing with his knowledge and resourcefulness of the simulation software TOUGH2 and Zhibing Yang for his great teaching and assistance in the pre-course *Simulation of transport processes*, which has been very helpful in my preparations for this thesis. Last, but not least, I would like to thank Auli Niemi for her helpfulness, appreciated recommendations on literature and valuable reviews of this work.

The research leading to these results has received funding from the European Community's Seventh Framework Programme FP7/2007-2013 under grant agreement n° 227286, as part of the MUSTANG project.

Christofer Olofsson

UPTEC W 11 015, ISSN 1401-5765
Printed at the Department of Earth Sciences, Geotryckeriet, Uppsala University, Uppsala, 2011.

POPULAR SCIENCE REVIEW

Global warming has been known for decades and many researchers claim that it is anthropogenically caused by excessive emissions of carbon dioxide (CO_2). The proposed reason to anthropogenic cause global warming is enhancement of the greenhouse effect, which is a naturally occurring phenomenon that can be observed on any planet with an atmosphere. Water vapor, methane and CO_2, are a few examples of significant gases in the atmosphere creating the greenhouse effect. Fossil fuels are highly concentrated sources of stored energy from previous sunlight that no longer have a role in our ecosystem. The energy is stored through plants fixating the carbon from the CO_2 in the atmosphere with the help of sunlight energy. By exploiting sources of fossil fuel, such as oilfields and coalmines, stored away CO_2 becomes reintroduced into our ecosystem, creating a shift in the eco balance leading to a warmer climate. Ever since the general acceptance of the global warming being anthropogenically affected, efforts have been made to reduce greenhouse gas emissions. Political incentives have been manifested in a convention known as the Kyoto Protocol and policies such as the introduction of CO_2 emission rights in Europe.

One solution for reducing the emissions of greenhouse gasses is to simply capture and store CO_2. The process is known as CCS (Carbon Capture and Storage). The capturing process is still considered to be energy demanding but hopefully ongoing research projects will be able to increase the effectiveness of the process within the near future.

Because the idea is to eliminate the excessive CO_2 in the earth atmosphere, the storage site has to offer a secure and cost efficient storage during indefinite time. A lot of options are available but only a few are provided with beneficial properties such as low maintenance costs and a hidden location. A few examples of storage sites that are considered suitable are depleted oil and gas reservoirs, unmineable coal seams and deep saltwater aquifers.

In order to optimize the usage of a storage site, the gas is compressed to such pressures that the gas reaches a different state of phase. Storing CO_2 under high pressure, the substance state of phase becomes super critical, which is somewhat similar to a liquid state. The benefit of compressing the CO_2 is that the density increases so that more CO_2 can be stored using less volume of the storage site. If the pressure is decreased, the super critical CO_2 ($scCO_2$) will return to its gaseous state of phase. This means that the storage site has to be located at such depth that the naturally occurring pressure and temperature assures a continued super critical state.

Not only is it important the storage site's temperature and pressure is right, but the storage site also has to have a layer on top of the storage formation that does not allow the $scCO_2$ to pass though. Such a layer is said to be impermeable and is also known as a cap rock, usually consisting of clay. The reason for the need of a cap rock is that super critical CO_2 has a lower density than water and therefore strives to float on top of the water that storage sites at such depths usually contain. Typical storage formations are saline sandstone aquifers overlain by low-permeability rocks.

Because the storage site might have cracks in its cap rock or because it simply ends at a certain distance, it is important to estimate how much $scCO_2$ can be injected before it reaches these escape points. In order to make an accurate estimation, one needs to estimate the possible migration of the CO_2. The migration depends on the storage site's material properties and how they change within the aquifer. Key properties that have an impact on the migration pattern are

the *average permeability* (the measure of how fast fluids can travel through the material) *variance* of the permeability (highest and lowest measured value) and the *covariance,* which can be described as the likelihood that two neighboring points have the same permeability. Spatial variation in the permeability is part of what is referred to as heterogeneity.

This study sets out to describe how heterogeneity affects the distribution of geologically stored CO_2 by using sampled data from a deep saline aquifer named Heletz, which is located in Israel. By creating mathematical models describing the heterogeneity, based on the Heletz aquifer core samples, a large number of equally probable scenarios of heterogeneity can be created. When simulating an injection into each created scenario, one can estimate the most likely outcome. This method is called the Monte Carlo method and is a good way to simulate systems with a lot of uncertainties. In this case, the lack of knowledge about the heterogeneity outside the small number of core samples is the reason for uncertainties. This study does not try to simulate the actual aquifer of the Heletz aquifer but instead tries to look at tendencies of the $scCO_2$ distribution within its material with the presence of heterogeneity in permeability. Therefore the goal in this study is to provide a better understanding of the significance that heterogeneity in permeability have for the CO_2 distribution.

The results in this study show that a higher permeability in the storage formation can result in less storage efficiency. This is because a higher permeability leads to more influence of buoyancy on the spreading, more CO_2 accumulation directly under the formation ceiling and, thus, a larger horizontal migration distance. The study shows that a larger variance in permeability within the aquifer reduces the aquifer's possibility to store large amounts of CO_2 because of longer horizontal migration. Also, the results show that an increased horizontal correlation length decreases the storage capacity.

POPULÄRVETANSKAPLIG SAMMANFATTNING

Global uppvärmning har varit känd i årtionden och många forskare hävdar att den är antropogent orsakad genom stora utsläpp av koldioxid (CO_2). Den föreslagna anledningen till är den så kallade växthuseffekten vilket är ett naturligt förekommande fenomen för planeter med atmosfär. Vattenånga, metan och CO_2 är några exempel på gaser i atmosfären som skapar växthureffekten. Fossilt bränsle är högt koncentrerade källor av lagrad energi från tidigare solenergi som träffat jorden och som genom lagring inte längre ingår i jordens ekosystem. Energin lagras genom att växtriket fixerar kol från atmosfärens CO_2 med hjälp av solenergi. Genom exploatering av dessa källor återinförs den lagrade koldioxiden och på så sätt förskjuts atmosfärens balans vilket i sin tur leder till ett varmare klimat. Försök att reducera utsläppen av växthusgaser har gjorts sedan det blev allmänt erkänt att den globala uppvärmningen till viss har antropogen orsak. Politiska incitament har manifesterats i en konvention känd som Kyotoprotokollet och politiska styrmedel som utsläppsrätter i Europa.

En lösning för att minska utsläppen av växthusgaser är helt enkelt att fånga och lagra CO_2. Processen är känd som CCS (Carbon Capture and Storage). Själva processen att separera CO_2 från utsläppen anses fortfarande vara energikrävande, men förhoppningsvis kan pågående forskning öka processens effektivitet inom en snar framtid.

Eftersom idén är att avlägsna den överflödiga CO_2 från atmosfären är det extra viktigt att lagringsplatser kan erbjuder säker och kostnadseffektiv lagring på obestämd tid. Det finns en hel del alternativ tillgängliga men endast ett fåtal med fördelar som låg underhållningskostnader och undangömd lagring. Exempel på sådana lagringsplatser är exploaterade olje- och gasreservoarer, djupt belägna kollager och djupt belägna saltvattenakvifärer.

För att optimera användandet av en lagringsplats komprimeras CO_2 i dess gasform för att på så sätt skapa en ökning i dess densitet. Genom högt tryck och rätt temperatur kan nämligen CO_2 nå ett tillstånd mellan gas och flytande. Man säger då att CO_2 befinner sig i ett superkritiskt tillstånd ($scCO_2$). Ökat tryck leder med andra ord till en högre mängd CO_2 per volymenhet och på så sätt kan mer CO_2 lagras inom samma lagringsutrymme. Om trycket inte är tillräckligt högt riskerar CO_2 att övergå från dess superkritiska tillstånd till gasform igen vilket i sin tur ökar risken för läckage till atmosfären. Därför är det viktigt att lagring sker på sådant djup att tryck och temperatur är tillräckligt högt för att garantera en fortsatt lagring av CO_2 i dess superkritiska tillstånd.

Det är inte enbart viktigt att undersöka en lagringsplats tryck och temperatur utan en lämplig lagringsplats behöver även ett lager ovanpå lagringsformationen som förhindrar att $scCO_2$ kan spridas uppåt. Ett sådant lager benämns som ett impermeabelt topplager och består ofta av lera. Anledningen till att ett sådant topplager behövs är att $scCO_2$ har en lägre densitet än akvifärens vatten och därför strävar efter att flyta ovanpå vattnet i akvifärer. Typiska lagringsformationer är salina saltvattenakvifärer med ett impermeabelt topplager av lera.

Eftersom lagringsplatsen kan ha sprickor i topplagret, eller helt enkelt upphör efter ett visst avstånd, är det viktigt att estimera den maximala mängden CO_2 som formationen kan lagra. För att göra en tillförlitlig uppskattning behöver en mängd faktorer tas med i beräkningarna. En sådan faktor är till exempel koldioxidens benägenhet att spridas i lagringsmaterial. Koldioxidens benägenhet till spridning beror av lagringsmaterialets egenskaper och även hur dessa egenskaper skiljer sig mellan olika platser i lagringsformationen. Exempel på sådana

egenskaper är den *genomsnittliga permeabilitet* (mått för hur snabbt fluider kan färdas genom porösa material), *varians* i permeabilitet (högsta och lägsta värde) samt covarians (sannolikheten att två närliggande punkter har samma permeabilitet). Heterogenitet är ett begrepp som bland annat omfattar skiftande egenskaper i permeabilitet.

Denna studie beskriver hur heterogenitet påverkar distributionen av geologiskt lagrad CO_2 med hjälp av tidigare insamlad brunnsdata. Denna data kommer från en djupt belägen saltvattenakvifär vid namnet Heletz, Israel. Matematiska modeller användes för att beskriva Heletz uppskattade heterogenitet och genom detta kunde ett flertal möjliga utfall vid injektion av CO_2 undersökas. Metoden kallas för Monte Carlo Metoden och är bäst lämpad vid simulering av system med många osäkerheter. I denna studie är det just mängden mätdata som utgör den stora osäkerheten. Denna studie försöker inte simulera den faktiska akvifären i Heletz område. Studien undersöker istället spridningen av scCO_2 vid injektion i material med heterogena förhållanden i permeabilitet. Syftet med denna studie är därför att ge en bättre förståelse för betydelsen av heterogenitet i permeabilitet för distributionen av CO_2.

Resultaten i denna studie visar att en högre permeabilitet i lagringsformationen kan orsaka minskad lagrings effektivitet. Den högre permeabiliteten leder till spridningen av CO_2 får en större influens av flyteffekt, en högre ansamling under formationens tak och därmed en längre horisontell spridning. Studien visar även att en större varians i permeabilitet reducerar akvifärens möjlighet att lagra stora mängder CO_2 på grund av lång horisontell spridning. Slutligen, resultaten indikerar att ökad horisontell korrelationslängd orsakar minskad lagringseffektivitet.

TABLE OF CONTENT

LIST OF FIGURES

LIST OF TABLES

1 INTRODUCTION

Carbon dioxide has certainly been an ongoing topic of discussion ever since the increased greenhouse effect became known. Debates have taken place whether the global warming is anthropogenically caused and in 2007 the Intergovernmental Panel on Climate Change (IPCC) released a report suggesting it being very likely that human activities, such as carbon dioxide emissions from fossil fuel, are contributing to the rapid increase of the average temperature around our planet (IPPC, 2007). In order to reduce the anthropogenically caused effect the main goal is to decrease the emissions of carbon dioxide (CO_2) to the atmosphere. Countries that agreed to the Kyoto Protocol are assigned a quantity of emission units. Those who do not use their full share can sell the excess units to those unable to stay within assigned limits of emission. This is known as Emission Trading where enterprises such as energy companies and production industries trade emission rights on a daily basis (UNFCC, 2011-01-09). Because the emissions of CO_2 are adding to the cost of production, an incentive for reducing emissions has formed and even opened up the possibility to increase profits by selling emission rights if the reduction is successful. In order to do so, an effective technique to capture as well as store CO_2 is crucial.

Aquifers located deep underground are subject for research as possible hosts for large scale storage of CO_2. The main advantage of this type of storage, geological storage, is the large storage capacity and already existing storage space at a hidden location. Depending on the temperature and pressure the CO_2 can be held in a super critical state of phase[1]. By compressing the CO_2 after separation from various emission sources, the gas can be injected into an aquifer located at such depth that the naturally occurring pressure and temperature enables the CO_2 to be stored in a supercritical state (IPPC 2005).

When injecting CO_2 into an aquifer, a number of aspects need to be taken into account. When planning an injection of CO_2 into an aquifer one needs to account for the distribution of the supercritical CO_2 ($scCO_2$) after the injection phase. How the injected $scCO_2$ will be distributed largely depends on the properties of the aquifer, such as permeability, porosity, compressibility and heterogeneity in these properties. One way to determine the material properties of the site is through core sample testing. Since drilling at a large depth is both time consuming and extremely expensive in heterogeneous systems, a computational approach for estimating the CO_2's distribution based on limited core samples is through stochastic simulation.

Several studies concerning geological storage in deep saline aquifers have been carried out. Doughty and Pruess (2004) and Flett et al. (2007) write that numerous studies have emphasized on geological storage of CO_2 with idealized geological representation. Doughty and Pruess (2004) investigate the physical processes that occur when storing CO_2 in a saline water-saturated geological formation. Different from many previous studies, in idealized geological settings, they set out to investigate the effects of grid resolution, grid orientation and characteristic curves in a strongly heterogeneous setting. In particular, they look at the significance of geologic heterogeneity from a capacity point of view by using realistic variability.

[1] Super critical is a state of phase different from gas, liquid and solid. The super critical phase of CO_2 has a higher density compared to its gaseous state enabling large amounts of CO_2 to be stored.

Flett et al. (2007) showed that heterogeneity has a large impact on the migration behavior of CO_2 by using fictitious geological marine sand models in their study.

Another study with a full-scale 3D model concerning a deep saline aquifer is Hovorka et al. (2004). They developed a reservoir model for the Frio Formation. Among other things, their study shows that residual CO_2 saturation is a significant source of uncertainty during storage. A higher residual saturation gives a limited spread of the CO_2 plume and if the injected CO_2 moves through high-permeable pathways, it will reduce the residual trapping.

The objective of the present study is to carry out simulation studies addressing the effect of heterogeneity based on well-log and core-sample data from the CO_2 injection test site Heletz. Heletz is the main CO_2 injection site of the EU FP7 project MUSTANG. The aim of this thesis is to contribute to a better understanding of how the reservoir properties *average permeability*, *variance in permeability* and *spatial correlation structure* influence the distribution of CO_2 within the deep saline aquifer target layer by simulating using iTOUGH2.

2 MATERIALS AND METHODS

2.1 HELETZ STORAGE SITE

The Heletz saline aquifer is located in Israel and is subject for CO_2 test injections in the EU project MUSTANG. Heletz was extensively investigated for crude oil where findings were made in some regions and later exploited. Injection of CO_2 is planned to be made at a location where no oil was found. The envisaged storage layer is a sandstone material with an impervious clay layer on top of the sandstone hindering the CO_2 from migrating upward. The depth of the aquifer is a key ingredient since the pressure at 1500 meter is sufficient for keeping the injected CO_2 in its super critical state.

Heletz storage site consists of layers within its target layer. The layers used between each impermeable layer are named K, W and A. The impervious layers were not taken into account in this thesis as illustrated in Figure 1.

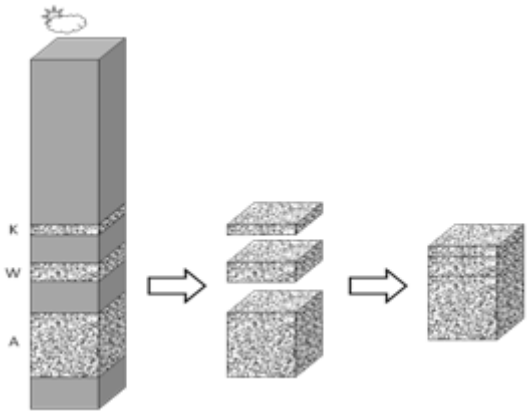

Figure 1 Illustration of the three layers being used as one layer, variance between the layers is not taken into account, only the variance within each layer.

Figure 2 is a map over Heletz storage site with a close up view on the area in which the injection well (H18) and the two observation wells (H13 and H38) are located. The mentioned wells are those that the well log data, used in this thesis, were collected from (courtesy of Shtivelman, V. GII, Israel).

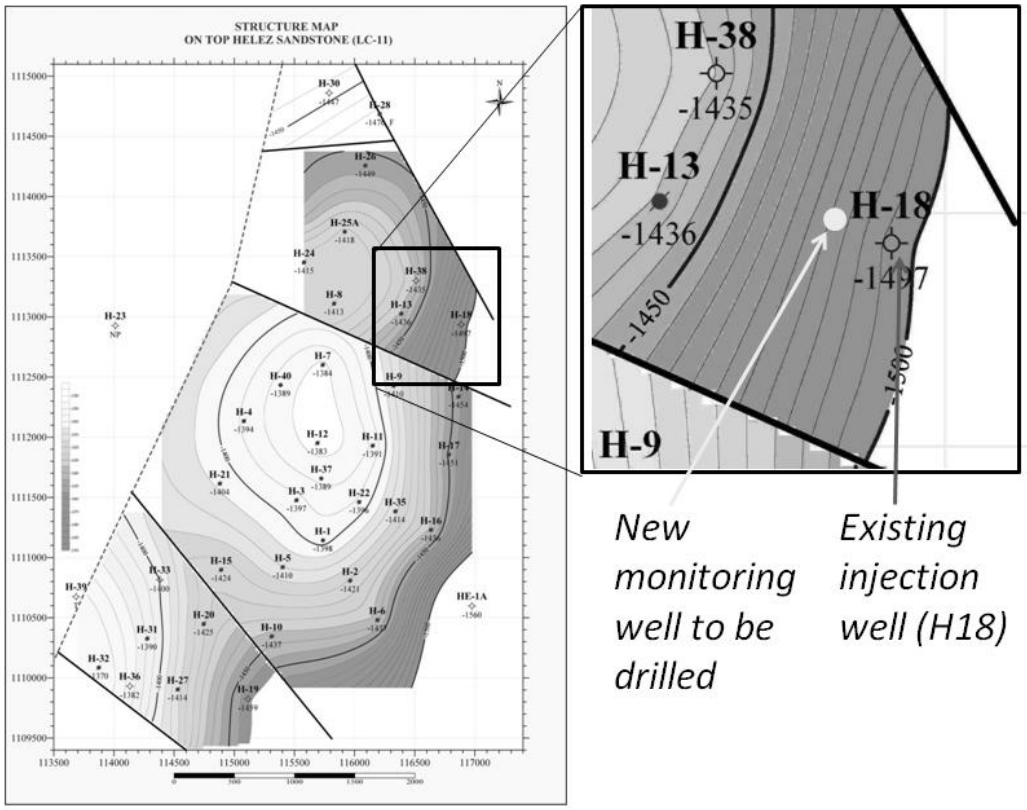

Figure 2 Map over Heletz test site (Fagerlund et al., 2010).

The well log measurements are available at 10 cm spacing in the bore holes. Core samples were also collected in several places in many different wells. Measurements of porosity and permeability for these core samples have allowed the formulation of a relationship between porosity and permeability, specifically for the Heletz sandstone target layer (courtesy of Shtivelman, V. GII, Israel).

$$k = 0.006 * e^{(0.5\emptyset)} \quad (1)$$

where:
$k = permeability\ [mD]$
$\emptyset = Porosity\ [\%]$

The well logs of porosity were used together with this relationship (Equation 1) to map the vertical distribution of permeability in the bore holes. These data allowed determination of a semivariogram in vertical but not horizontal direction. ***Error! Reference source not found.*** shows the thickness of each layer contributing to sample data of the sandstone and the number of well log measurements available from each layer.

Table 1 Thickness, d_i, of target layers (i=A, K, W) and the number of samples (n_i) for each layer.

Well	**Thickness of layers and number of measurements**					
	d_K(m)	**n_K**	**d_A(m)**	**n_A**	**d_W(m)**	**n_W**
H18	1.2	13	1.1	13	6.7	47
H13	0.4	5	0.7	8	4.7	48
H38	1.6	17	2.8	29	4.6	47

2.2 SEMIVARIOGRAM ANALYSIS

In order to mathematically describe the spatial correlation structure within the sandstone material, an experimental semivariogram was determined. An experimental semivariogram is an empirical estimate representing the variation in permeability of the storage material as a function of the distance between two points in a certain direction. The shorter the distance between two measuring points, the higher the probability is that the measured points have equal values. The expected variation in a parameter, as a function of separation distance (h), is typically described by semivariogram $\gamma(h)$ (de Marsily, 1986 and Niemi, 1994):

$$\gamma(h) = \frac{1}{2}E[(Z(x+h) - Z(x))^2] \quad (2)$$

where:
$\gamma = Semivariogram$
$E = expected\ value$
$Z = random\ value, observed\ value$
$x = position\ vector$
$h = distance\ bewteen\ two\ points$

Sorting the obtained core sample permeability data by depth and layer made it possible to determine $\gamma(h)$ by arranging the data from the three wells as one long core sample. The objective is to identify the geostatistical properties within the formation's storage material. Therefore $\gamma(h)$ was not calculated between the layers due to significant differences in average permeability which indicates on different statistical populations.

Figure 3 illustrates an example of 10 sampled values Z evenly separated by distance h meter. γ was calculated, according to Equation 2, for each distance h and the procedure was repeated in order to create a γ for each lag distance h.

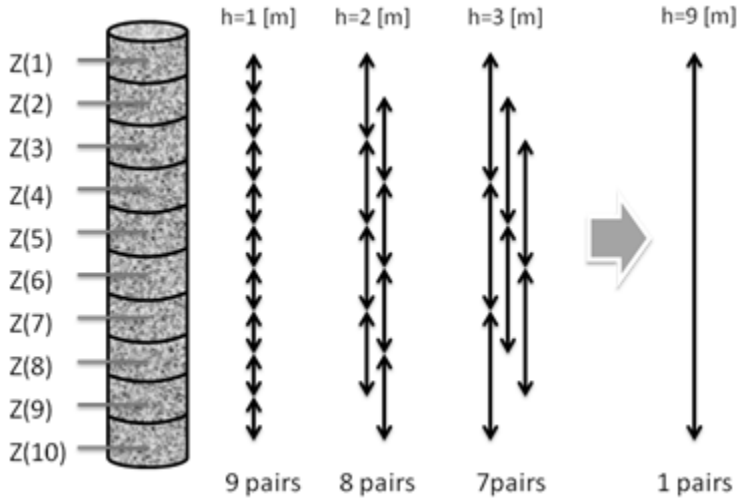

Figure 3 Demonstration of the amount of well log data pairs for different lag distances.

Note that the number of pairs decrease as distance h increase, resulting in a γ based on fewer data pairs as illustrated in Figure 3. Therefore γ that are based on a higher amount of data pairs should be honored (UNCERT, 2011-03-13).

The distribution of the permeability is often assumed to follow a log-normal distribution. For such a distribution a log-semivariogram is suitable which is created by log-transforming the permeability data before calculating semivariogram (γ) for each lag distance as described above (UNCERT, 2011-03-13).

After the procedure of calculating each value of γ, for the selected distances h, the results were plotted in order to fit an appropriate model describing $\gamma(h)$. Commonly used models are the exponential, spherical or the Gaussian model which are illustrated in Figure 4.

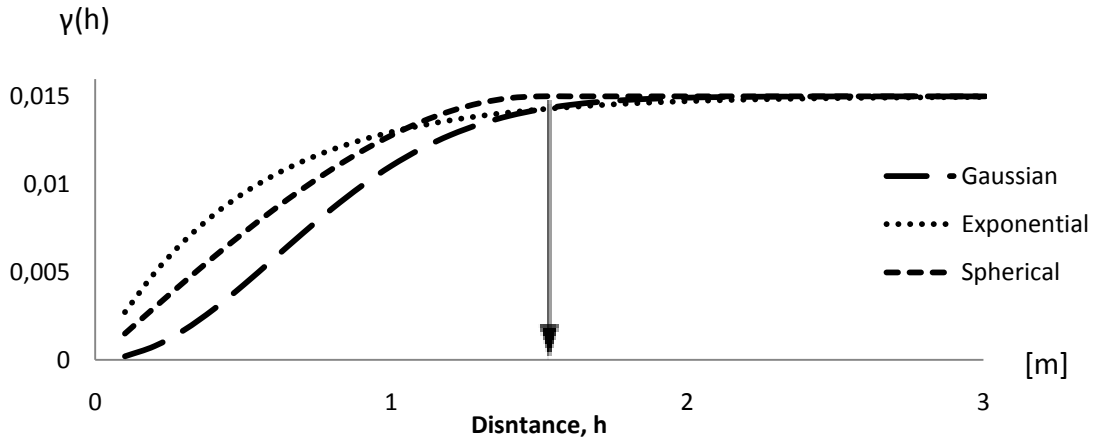

Figure 4 Illustration of commonly used models to describe the semivariograms.

The functional forms of these models are (de Marsily, 1986 and Niemi, 1994):

Gaussian
$$\gamma(h) = C_0 + \omega\left(1 - \exp\left(-\left(\frac{h}{a_g}\right)^2\right)\right) \tag{3}$$

Spherical
$$\gamma(h) = C_0 + \omega\left[\frac{3}{2}\left(\frac{h}{a_s}\right) - \frac{1}{2}\left(\frac{h}{a_s}\right)^3\right] \qquad h < a_s$$
$$\gamma(h) = C_0 + \omega \qquad h > a_s \tag{4}$$

Exponential
$$\gamma(h) = C_0 + \omega\left[1 - \exp\left(-\frac{h}{a_e}\right)\right] \tag{5}$$

where:
C_0 = nugget factor
ω = sill
h = length of vector h
a = parameter describing the semivariogram range

The nugget factor determines the minimum value of $\gamma(h)$, while the *sill* determines the maximum value. Parameter a does not always correspond to the correlation length. Each depends on the model being used to describe the semivariogram. Figure 4 also illustrate how the models fit differently for the same correlation length and sill. In the example figure the correlation length is 1.5m (illustrated by arrow) and the sill is 0.015. Only the spherical model, among the ones illustrated, has the relationship 1:1 between a_s and correlation length. In the exponential model, the correlation length is three times a_e. The correlation length is defined as the separation distance for which 95% of the sill value is reached. For the Gaussian model the correlation length is given by $a_g\sqrt{3}$. Therefore the Gaussian model has a a_g parameter of 0.866, the exponential model a a_e parameter of 0.5 and the spherical model a a_s parameter of 1.5 in order to describe the same correlation length of 1.5m (de Marsily, 1986, and as shown in Figure 4).

For the data in question, the semivariogram can only be determined in the vertical direction. In horizontal direction, the distance is too large to determine the semivariogram. In this study the vertical semivariogram was also used to estimate the horizontal correlation structure.

2.3 NUMERICAL MODEL

2.3.1 TOUGH2, iTOUGH2 and ECO2N

The numerical models used for simulating CO_2 spreading are the following:

TOUGH2 handles nonisothermal flows of multicomponent, multiphase fluids in all three dimensions. The software was first and foremost developed for simulation runs of geothermal reservoir engineering, nuclear waste disposal, environmental assessment and remediation (Pruess et al. 1999). Developments of the simulator have made it possible to simulate geologic storage of CO_2 through the module ECO2N.

iTOUGH2 is based on TOUGH2 and has additional features such as a Geostatistical Software Library making is possible to assign each element with a specific permeability following a spatially correlated stochastic distribution. The developed semivariogram parameters discussed in Chapter 2.2 can be used as input parameters to create random realizations with certain geostatistical properties thus making is possible to utilize the Monte Carlo model. (Finsterle and Kowalsky, 2007)

ECO2N is a module adding component properties to TOUGH2. A multi phase flow simulation of water, salt and carbon dioxide can be made by using the existing framework of TOUGH2's simulation resources and adding information on thermodynamics and thermophysical properties of the three components. ECO2N uses large tables of thermodynamic and thermophysical properties for within certain range and discretization to later interpolate the property data in order to obtain a more accurate value (Pruess, 2005). For further details the reader is referred to the User's manuals of the comprehensive codes.

2.3.2 Relative permeability and capillary pressure functions

iTOUGH2 gives the option to choose between a variety of functions describing relative permeability and capillary pressure. Specifically selected models and functions that were used in this work are listed below:

Brooks Corey - model (Brooks and Corey, 1964) is used.

$$P_c = P_d \bar{S}_L^{-\lambda} \quad (6)$$

where:

effective total liquid saturation, $\bar{S}_L$

$$\bar{S}_L = \frac{S_w + S_n - S_{wr}}{1 - S_{wr}} \quad (7)$$

$\frac{1}{\lambda}$ = *Pore-size distribution index*
P_c = *capillary pressure*
P_d = *air entry pressure*
$S_{wr} = residual\ water\ saturation$
$S_n = NAPL\ saturation$

$S_w = water\ saturation$

Relative permeability functions are described by from the Brooks Corey Burdine - model, described in Fagerlund et al. (2006), and are as follows:

Relative permeability for gaseous phase, k_{rg}

$$k_{rg} = CX_{rg}^2\left(1 - \bar{S}_L^{\,1+2/\lambda}\right) \quad (8)$$

$$C = \left(1 + \frac{b}{P_g}\right) \quad (9)$$

where:
b = Klinkenberg b-factor
P_g = pressure in gaseous phase
X_{rg} = effective tortuosity factor for gaseous phase

Relative permeability for Non-Aqueous Phase Liquid (NAPL), k_{rn}

$$k_{rn} = X_{rn}^2\left(\bar{S}_L^{1+2/\lambda} - \bar{S}_w^{\,1+2/\lambda}\right) \quad (10)$$

where:
X_{rn} = effective tortuosity factor for NAPL phase

Relative permeability for liquid phase, k_{rw}

$$k_{rw} = X_{rw}^2\bar{S}_w^{\,1+2/\lambda} \quad (11)$$

where:
X_{rw} = effective tortuosity factor for liquid phase

2.3.3 Leverett scaling

Used to scale the air entry pressure (Equation 12) of each element according to the permeability of the element, this is an option of iTOUGH2 in combination with GSLIB. Leverett scaling is defined as the root of the ratio between two elements permeability being equal to the ratio between the elements air entry pressure, according to (Leverett, 1941):

$$\frac{P_{d_1}}{P_{d_2}} = \sqrt{\frac{k_1}{k_2}} \quad (12)$$

where:
$P_d = Air\ entry\ pressure$
$k = Permeability$

2.4 SIMULTION SETUP

A 2D setup of the Heletz aquifer at borehole H18 was chosen for this study. A 3D simulation is expected to have a higher accuracy since it takes all the dimensions for the distribution of CO_2 into account but would on the other hand have been more demanding from a computational point of view. As the objective of the present study is to get a preliminary understanding concerning the effects of heterogeneity, 2D simulations were utilized.

A single-well injection of 1 000 000 kg CO_2 with an injection rate of 5 000 kg/hour is planned at Heletz well H18 (or similar well in the eastern part of Heletz), which equals an injection period of 8.33 days. As mentioned, the 2D modeling approach used in this study does not represent the actual single-well CO_2 injection planned at Heletz. The CO_2 injection in this 2D model is equivalent to a line source in 3D which would result e.g. from a line of injection wells. In this thesis the injection rate is equivalent to a line source of 155kg $hour^{-1}m^{-1}$. The injection rate was chosen so that the resulting horizontal migration distance of the CO_2 plume, for a homogeneous permeability distribution, is approximately the same as that predicted for the planned single-well injection using a 2D-radial model for the same injection time of 8.33 days.

2.4.1 Monte Carlo approach

The Monte Carlo method is an approach used to simulate stochastic processes and was applied in this thesis. The method was utilized by creating multiple realizations[2] where an injection later was simulated for each realization. By simulating a large number of realizations, an expected outcome could be determined. This method is advantageous because it requires less deterministic assumptions compared to analytical methods but on the other hand demands a higher amount of computational resources.

The Monte Carlo approach can be conditional as well as unconditional. In this study the Monte Carlo approach chosen is unconditional which means that the created realizations are free from determined permeability values at specified coordinates. In other words, the realizations are statistically equal with random values at each coordinate in space (Niemi, 1994). The reason for using an unconditional approach is to obtain a result describing the general behavior of Heletz sandstone and similar sandstone materials.

Determination of the number of realizations depends on the observed output variations. Normally, realizations are generated and simulated for as long as significant changes of the distribution occur. However, this study limited its realizations for each case of heterogeneity to 40 because of scarce computer resources and limited time.

[2] Realizations, randomly distributed and unique permeability fields with equal geostatistical properties.

2.4.2 Outline of simulations

In order to investigate influence that the *average permeability*, *variance in permeability* and *horizontal correlation length* have on the distribution of CO_2, the simulation outline was constructed as described in Figure 5. Permeability is denoted as k, variance as sill, horizontal correlation length as H.C.L and vertical correlation length as V.C.L. Best estimate is denoted as B.E and represents the best estimates made for Heletz target layer based on the well log data.

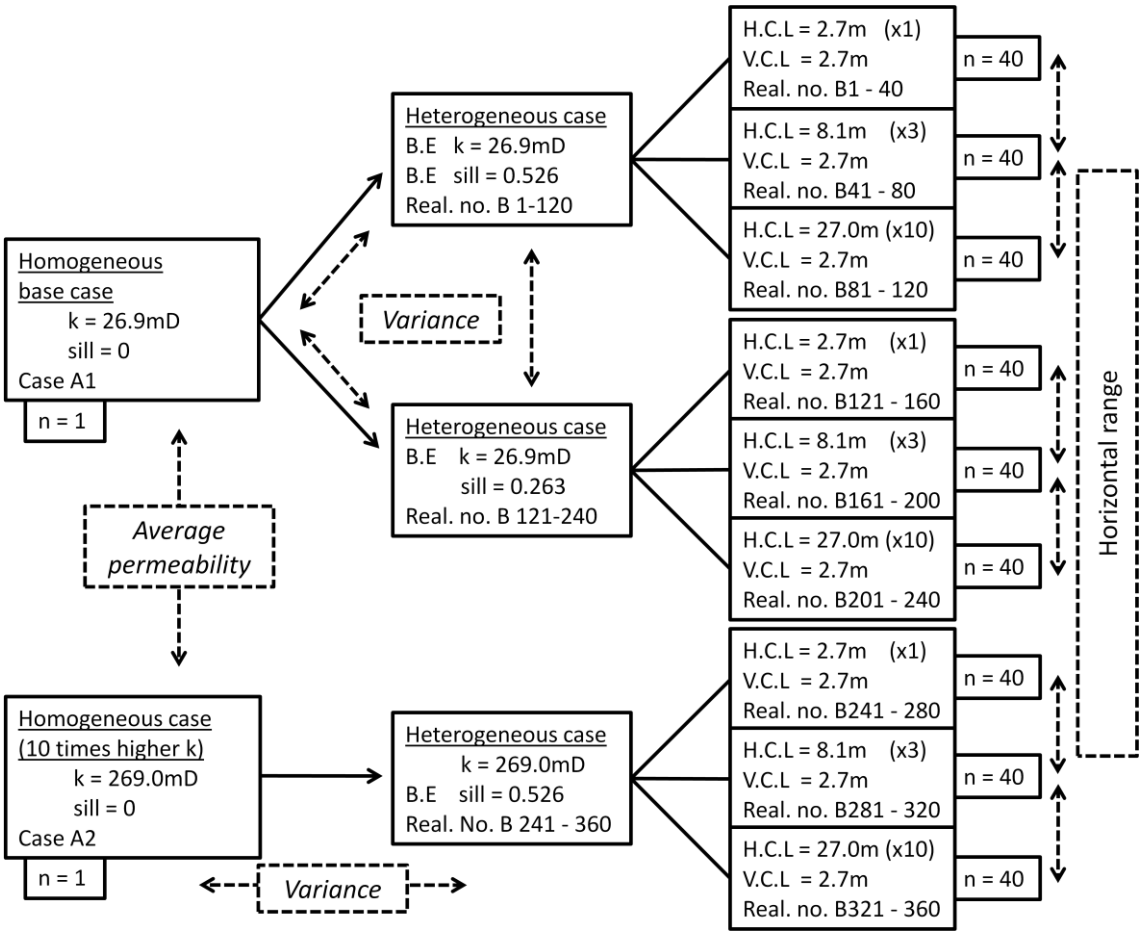

Figure 5 Flowchart of the simulation work

The first case investigated was the homogeneous base case that represents the B.E permeability (k). After simulating the base case, cases of heterogeneity were simulated. The B.E variance (sill) was investigated for the case of isotropy (H.C.L = V.C.L), small anisotropy (H.C.L = V.C.L x3) and large anisotropy (H.C.L = V.C.L x10). The V.C.L is constant through all cases and each case of different spatial correlation structure consists of 40 realizations throughout this thesis.

After investigations of the B.E cases, the B.E permeability with a smaller variance was investigated for different cases of heterogeneity. The heterogeneity cases were simulated with isotropy (H.C.L = V.C.L), small anisotropy (H.C.L = V.C.L x3) and large anisotropy (H.C.L = V.C.L x10).

A homogeneous case of high permeability (ten times higher than B.E) with B.E variance was also investigated in order to observe effects that the permeability might

have in comparison to the base case. The heterogeneity cases with small variance were simulated with isotropy (H.C.L = V.C.L), small anisotropy (H.C.L = V.C.L x3) and large anisotropy (H.C.L = V.C.L x10).

2.4.3 Discretization

Discretization is an important aspect when performing numerical simulations. A higher discretization is known to produce a more accurate result but with the downside of higher demand of computer capacity. Therefore, a higher resolution (discretization) was chosen around the injection well (see Figure 7) since that is the area where most activity occurred. Figure 6 shows the used measures when specifying the simulated aquifer. Note that the lines representing the discretization in Figure 6, Figure 7 and Figure 8 are incorrectly scaled and serves only as a schematic drawing with purpose to give the reader a sense of the discretization used. All the measurements shown in these figures are on the other hand exact.

Horizontally - the discretization varies. See Figure 2 and Figure 3 with following text for more detailed information.

Vertically - the aquifer consists of 20 elements all 0.5 meter high.

Depth - one element with the length of 1 meter.

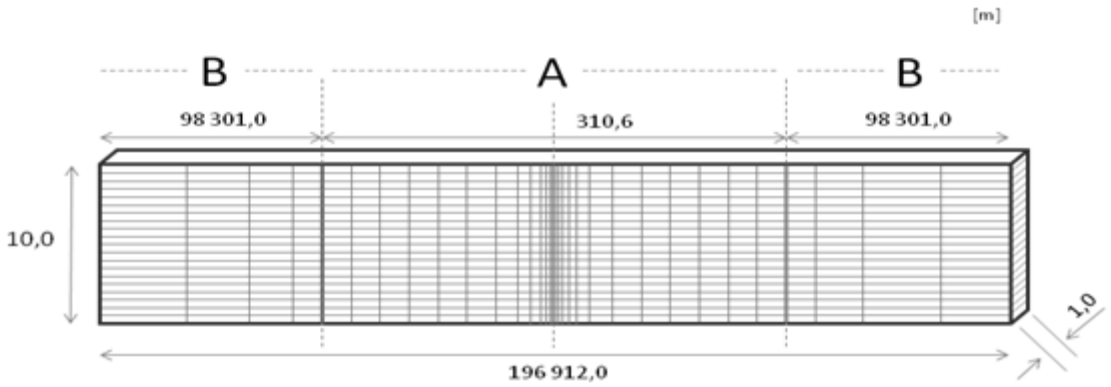

Figure 6 Schematic drawing over the modeled aquifer.

Volumetric measurements;
Section A: $310{,}6 * 1 * 10 = 3\,106 m^3$
Section B: $98\,301{,}0 * 1 * 10 = 983\,010 m^3$ (on both sides of section A)

Figure 7 show the elements width in consecutive order from the elements representing the well and all the way to the element size 3m. Thereafter the element size continues to be of the width 3 meter for the rest of section A. Section A is symmetric around the well and therefore the same measures are applied on the left side, see Figure 6.

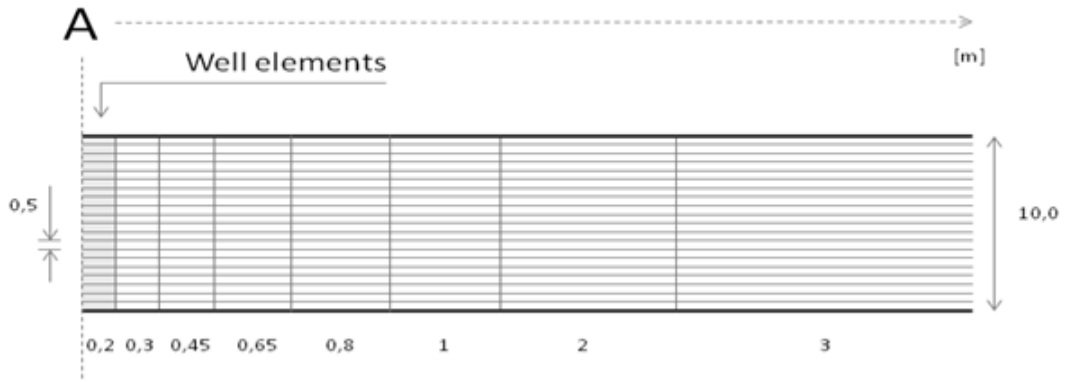

Figure 7 Schematic drawing over the modeled well and the close left side section A.

Figure 8 works in the same way as demonstrated in Figure 7 and show the discretization of section B. The modeled aquifer was designed with large end sections, B sections, in order to give the modeled aquifer the characteristics of infinity. The B section is also symmetrically represented on both sides of section A as shown in Figure 6.

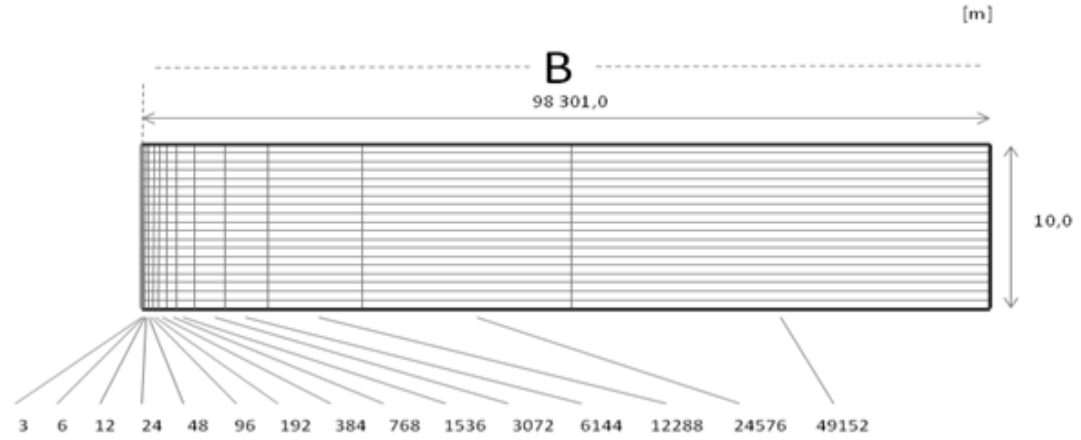

Figure 8 Schematic drawing on the right section B.

All boundaries around the modeled aquifer were set as no-flow boundaries which mean that no substance or increased pressure was able to leave through the aquifer's boundaries. The B sections of the modeled aquifer serves only as an infinite boundary to section A and never comes in contact with the injected supercritical CO_2 ($scCO_2$). Therefore section A has a much higher resolution mostly consisting of elements 1m high, 3m wide and 1m deep. Section B on the other hand exponentially increases in width.

Section B was not of the same high resolution but requires some discretization in order to represent an infinite aquifer. The boundary between section A and B would otherwise represent a constant boundary condition.

2.4.4 Definitions of evaluation criteria

A graphic evaluation of the simulation results is interesting to develop a sense of how the CO_2 distributes during the different cases of simulation. Since the Monte Carlo was utilized in this thesis, specific parameters used to analyze the simulation results were used in order to compare the different cases. The key parameters used to compare the results were; *Dissolved CO_2 in aqueous phase*, *Volumetric storage*, *Storage efficiency* and *Maximum migration distance*. Table 2 lists the definitions for these four key parameters used to analyze the simulation results.

Table 2 Definitions of evaluation criteria.

Name	**Definitions**
Dissolved CO_2 in aqueous phase	Total mass CO_2 dissolved in the aqueous phase in relation to the total mass $scCO_2$ injected.
Volumetric storage	The ratio of section A's volume containing $scCO_2$ and section A's total volume.
Storage efficiency	The ratio of total injected CO_2 mass and volume of formation pore space associated with the maximum spread of CO_2. For this 2D model, the latter volume is defined as: maximum CO_2 migration distance multiplied with depth, width and porosity of the target layer. $Storage\ efficiency = = \frac{Total\ injected\ mass\ CO_2}{Max.migration\ dist._{left+right} * Depth * Height * Porosity}$ (13)
Maximum migration distance	The maximum spread distance from the injection well.

3 RESULTS

The first step in describing the geostatic properties of the storage material is to investigate the most occurring permeability value and variation. Table 3 lists different statistical measures for the aggregate well-log data. The median permeability indicates that Heletz storage material has a low permeability and a high standard deviation indicating of a strongly heterogenic material.

Table 3 Statistics of aggregated core sample data from well H18, H13 and H38.

			Log transformed permeability data	
	Median Permeability [mD]	**Standard deviation [mD]**	**Median Permeability [log(mD)]**	**Standard deviation [log(mD)]**
Aggregated core data	26.916	114.414	1.430	0.725

3.1 PERMEABILITY DISTRIBUTION

A log transformation of the aggregated data shows that the permeability is of a log-normal distribution as illustrated in Figure 9.

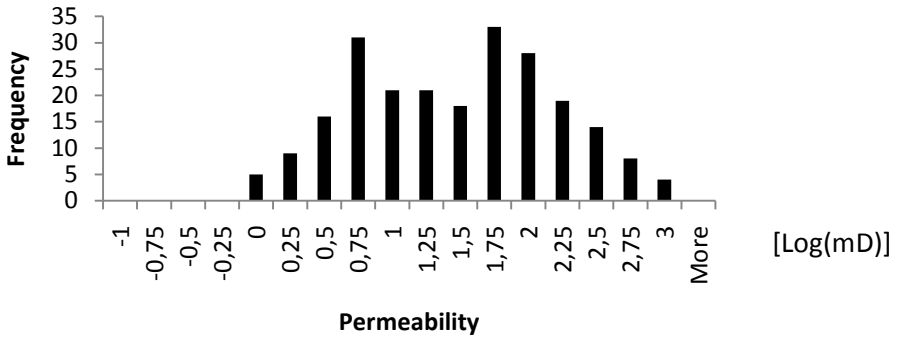

Figure 9 The log-normal distribution of aggregated data from well H13, H18 and H38.

3.2 SEMIVARIOGRAM ANALYSIS

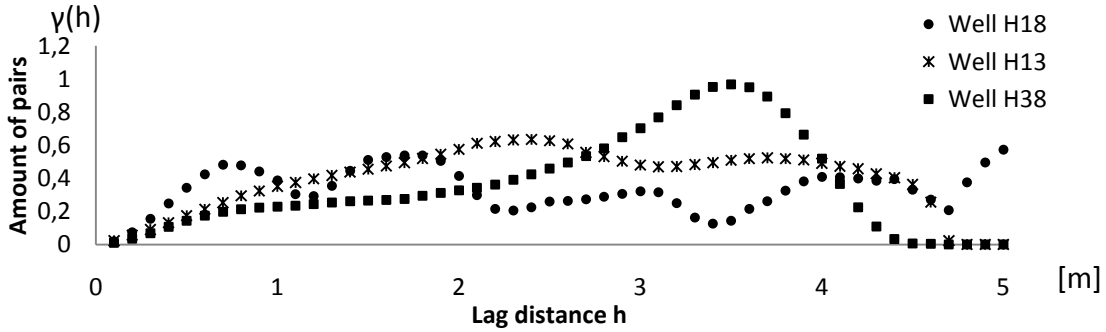

Figure 10 Log-semivariogram for well H18 and neighboring wells H13 and H38 separately.

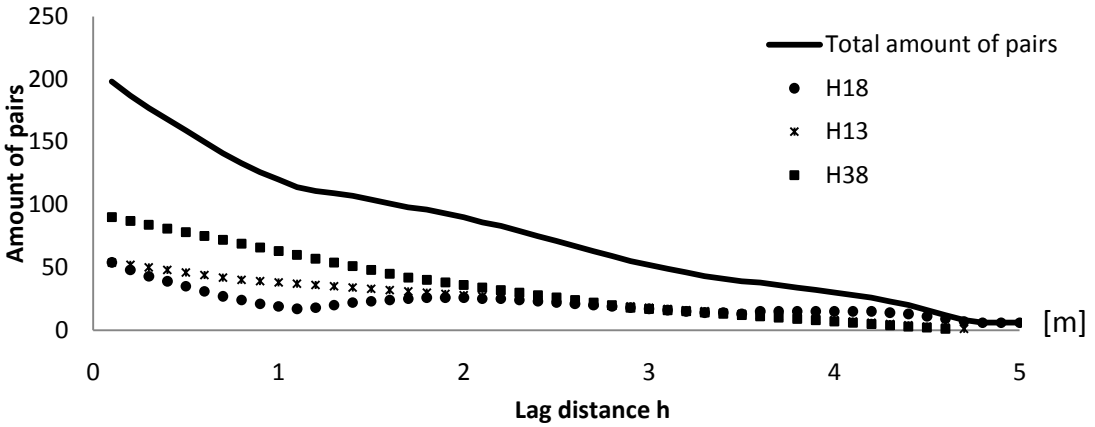

Figure 11 The amount of lag pairs for each lag distance.

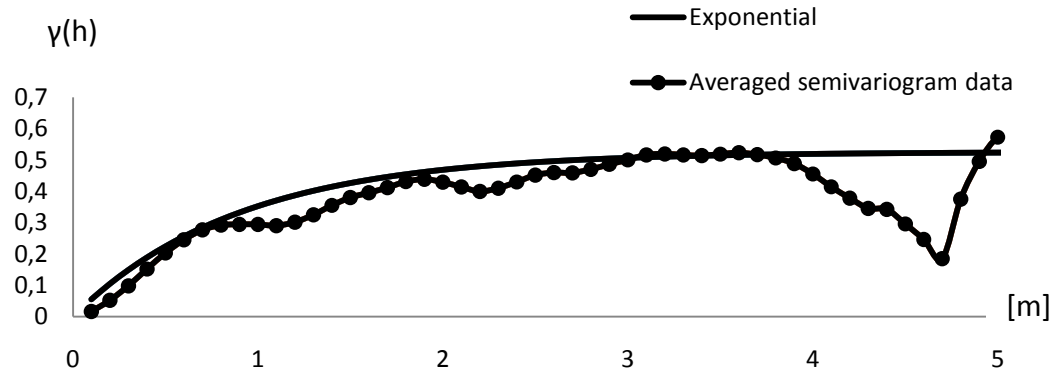

Figure 12 Log-semivariogram for combined well sample data fitted with the Exponential Model.

Figure 10 shows the log-semivariogram up to 5 meter. Figure 11 shows the amount of lag pairs that each core sample contributes as well as their aggregate amount. The figure does not show further data than 4meter due to the scarce amount of lag pairs that are considered too small to be usable. The exponential model described the log-semivariogram best and Figure 12 show how the log-semivariogram γ(h) converge towards = 0.526. The horizontal correlation length was determined to 2.7 meter which has a corresponding range parameter (a) of 0.9 for the exponential model. The nugget effect is assumed not to be present.

Table 4 Determined parameters for the fitting of the experimental model to the log-semivariogram

Model	a	Nugget factor	Sill
Exponential Model	0.9	0	0.526

The *sill* value was determined to 0.526 for two reasons;

1) Standard deviation for log-transformed aggregated core data = 0.725, as specified in Table 3.

$$sill = standard\ deviation^2 \quad (14)$$

$$=> sill = 0.526 \quad \text{(Barnes, 1991)}$$

2) Graphic fitting (see Figure 12)

The log-semivariogram correlation length was fitted graphically.

3.3 CASES WITH BEST ESTIMATE PERMEABILITY AND VARIANCE

In the following chapters (3.3.1 to 3.3.3) the results of the simulations with the best estimate permeability and variance (summarized in Figure 5) are presented. Chapter 3.3.1 show the homogeneous case of the best estimate permeability. Chapter 3.3.2 show the best estimate heterogeneous case with isotropic correlation lengths and Chapter 3.3.3 show the homogeneous case of large anisotropic correlation lengths.

Note that the figures in this chapter are plotted with such an aspect ratio that the y-axis increment is half as large as the x-axis. The reason is to make viewing easier by magnifying the plots in y-direction.

3.3.1 Homogeneous case with best estimate permeability

The super critical CO_2 ($scCO_2$) plume spreads evenly during the injection phase of the homogeneous base case (k = 26.9mD) as shown in Figure 13. A pronounced buoyancy effect can be observed after a redistribution period of 21.67 days (Figure 14).

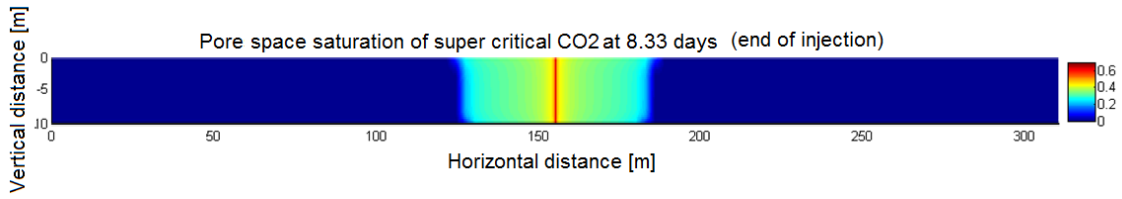

Figure 13 Super critical CO_2 saturation at 8.33 days of injection.

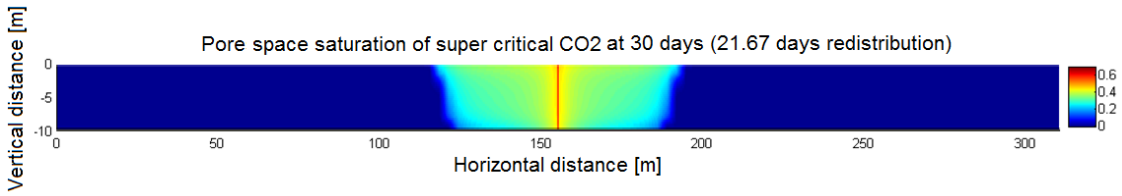

Figure 14 Super critical CO_2 saturation at 30 days including 8.33 days injection.

3.3.2 Heterogeneous case, best estimate of permeability and variance with isotropic correlation lengths

Figure 15 illustrates one realization of the permeability field for the best estimate permeability as well as best estimate variance. The horizontal correlation length (H.C.L) is equal to the vertical correlation length (V.C.L) (k = 26.9mD, sill = 0.526, H.C.L = 2.7m and V.C.L = 2.7m). The distribution of the $scCO_2$ plume does not indicate that the buoyancy effect is significantly dominating. The distribution is instead more affected by the variance and spatial correlation structure of the storage material (Figure 16).

The buoyancy effect is not significantly large after a 21.67 day redistribution period. Also, the $scCO_2$ plume spreads irregularly and migrates further through high permeable pathways (Figure 17).

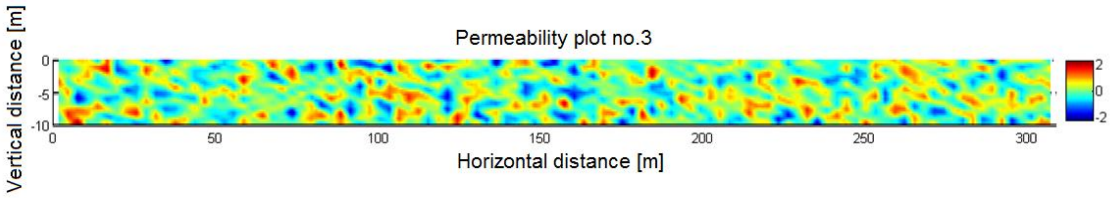

Figure 15 Example permeability field for best estimate permeability, best estimate variance and isotropic correlation lengths (realization B3).

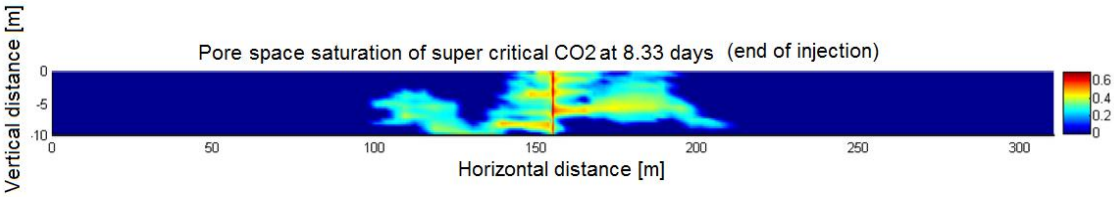

Figure 16 Super critical CO_2 saturation at 8.33 days of injection.

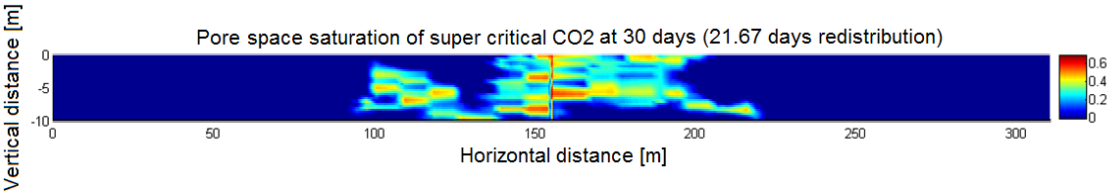

Figure 17 Super critical CO_2 saturation at 30 days including 8.33 days injection.

3.3.3 Heterogeneous case, best estimate of permeability and variance with anisotropic correlation lengths

Figure 18 illustrates one realization of the permeability field for the best estimate permeability as well as best estimate variance. The H.C.L is ten times longer than the V.C.L (k = 26.9mD, sill = 0.526, H.C.L = 27m and V.C.L = 2.7m).

Long high permeable pathways in the horizontal direction are observed in this case due to large anisotropy in correlation lengths (Figure 18). The high permeable pathways are having a significantly larger effect on the distribution of $scCO_2$ than the buoyancy effect, resulting in a significantly increased horizontal migration of $scCO_2$ though the high permeable pathways (Figure 19).The buoyancy effect is still not significantly large after a redistribution period and the high permeable pathways are still having a larger effect on the distribution of the $scCO_2$ plume. (Figure 20).

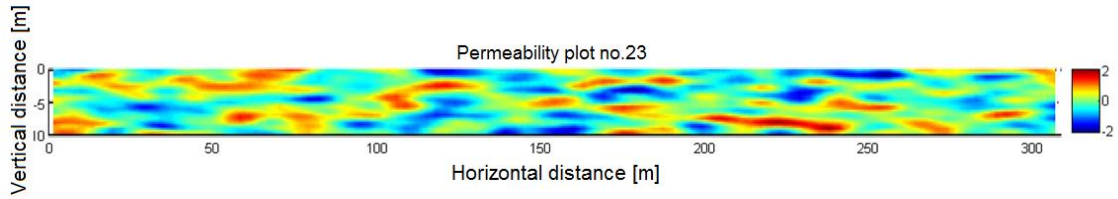

Figure 18 Example permeability field for best estimate permeability, best estimate variance and large anisotropy in correlation lengths (realization B103).

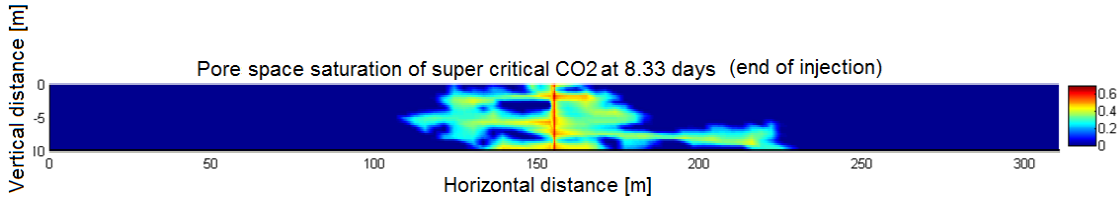

Figure 19 Super critical CO_2 saturation at 8.33 days of injection.

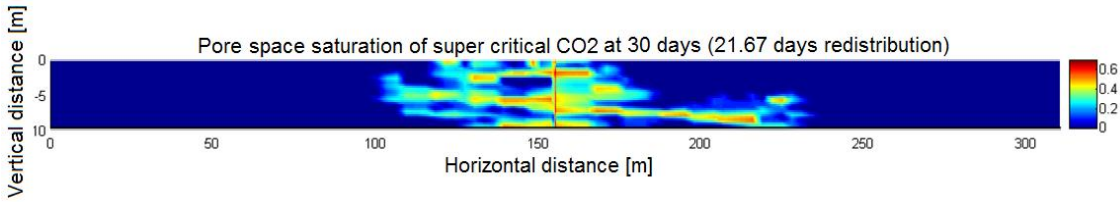

Figure 20 Super critical CO_2 saturation at 30 days including 8.33 days injection.

3.4 EFFECT OF VARYING THE ESTIMATED PARAMETERS

Note that the figures in this chapter are plotted with such an aspect ratio that the y-axis increment is half as large as the x-axis. The reason is to make viewing easier by magnifying the plots in y-direction.

3.4.1 Heterogeneous case, best estimate of permeability with low variance and isotropic correlation lengths

Figure 21 illustrates one realization of the permeability field for the best estimate permeability with low variance and isotropic correlation length (k = 26.9mD, sill = 0.263, H.C.L = 2.7m and V.C.L = 2.7m). The distribution of the $scCO_2$ plume does not show signs of a strong buoyancy effect right after the injection phase. At this stage the distribution is instead determined more by the variance and spatial correlation structure of the storage material (Figure 22). After a redistribution period on the other hand, the buoyancy effect is still visible at the same time as the spatial variation in permeability has a significant effect (Figure 23).

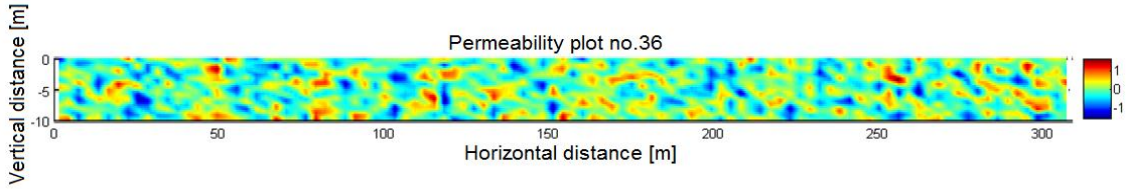

Figure 21 Example permeability field for best estimate permeability, low variance and isotropic correlation lengths (realization B156).

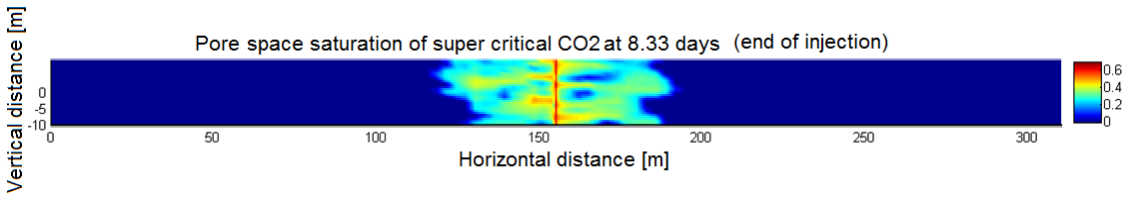

Figure 22 Super critical CO_2 saturation at 8.33 days of injection.

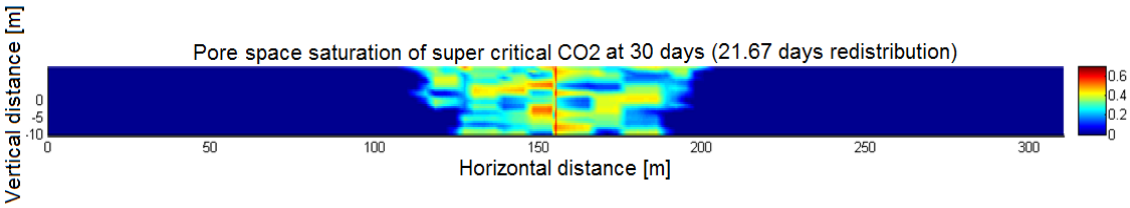

Figure 23 Super critical CO_2 saturation at 30 days including 8.33 days injection.

3.4.2 Heterogeneous case, best estimate of permeability with low variance and an isotropic correlation lengths

Error! Not a valid bookmark self-reference. illustrates one realization of the permeability field for the best estimate permeability with low variance. The H.C.L is ten times longer than the V.C.L (k = 26.9mD, sill = 0.263, H.C.L = 27m and V.C.L = 2.7m). In this case, long high permeable pathways in the horizontal direction are observed due to large anisotropy in correlation lengths (Figure 24). Migration through high permeable pathways as well as a buoyancy effect is observed right after the injection phase (

Figure 25). The buoyancy effect is still observable after a redistribution period but the high permeable pathways are having a significantly larger effect on the migration of the $scCO_2$ (

Figure **26**).

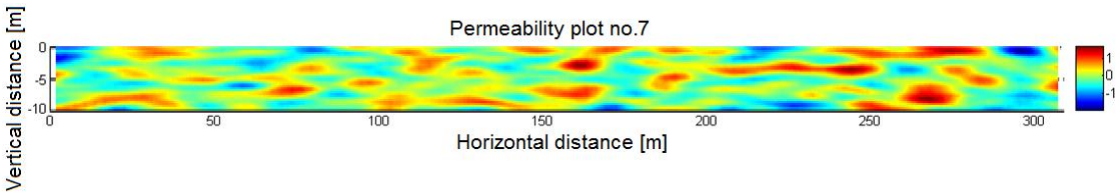

Figure 24 Example permeability field for best estimate permeability, low variance and large anisotropy in correlation lengths (realization B207).

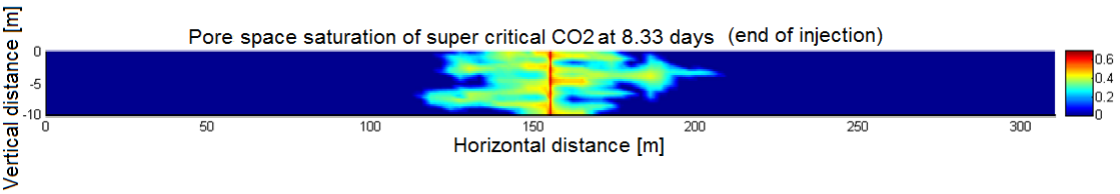

Figure 25 Super critical CO_2 saturation at 8.33 days of injection.

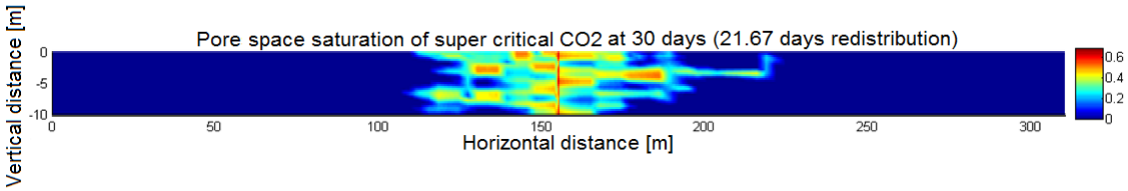

Figure 26 Super critical CO_2 saturation at 30 days including 8.33 days injection.

3.4.3 Homogeneous case of high permeability

The $scCO_2$ plume spreads evenly around the injection well in the homogeneous case of high permeability (k = 269mD) as shown in Figure 27. As expected in the case of higher permeability, the $scCO_2$ plume shows strong signs of a buoyancy effect after a 21.67 days log redistribution period (Figure 28**Figure *14***).

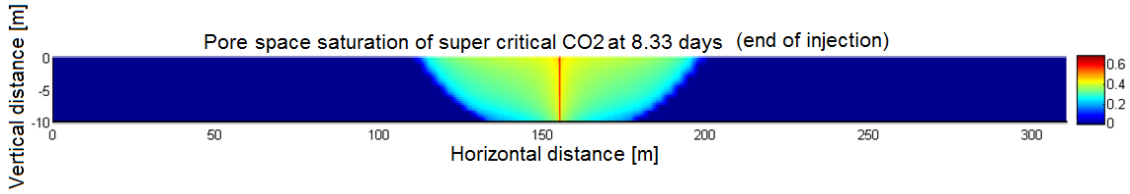

Figure 27 Super critical CO_2 saturation at 8.33 days of injection.

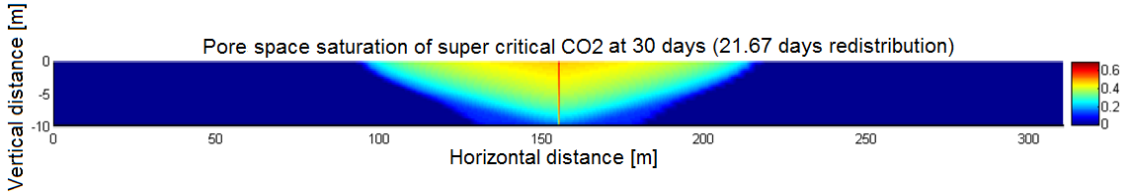

Figure 28 Super critical CO_2 saturation at 30 days including 8.33 days injection.

3.4.4 Heterogeneous case, high permeability and best estimate variance with isotropic correlation lengths

Figure 29 illustrates one realization of the permeability field for the best estimate variance with high permeability and isotropic correlation lengths (k = 269mD, sill = 0.526, H.C.L = 2.7m and V.C.L = 2.7m). At the end of injection, the distribution of the $scCO_2$ plume was strongly affected by the buoyancy effect at the same time as the $scCO_2$ was unevenly distributed due to spatial variation in permeability (Figure 30). Also, the $scCO_2$ plume migrated significantly longer along the top of the aquifer after a redistribution period (Figure 31).

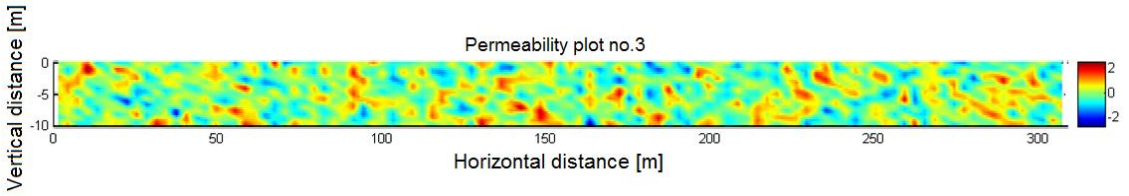

Figure 29 Example permeability field for high permeability, best estimate variance and isotropy in correlation lengths (realization B243).

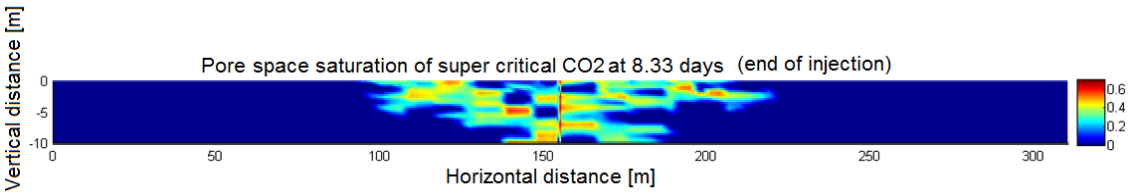

Figure 30 Super critical CO_2 saturation at 8.33 days of injection.

Figure 31 Super critical CO_2 saturation at 30 days including 8.33 days injection.

3.4.5 Heterogeneous case, high permeability and best estimate variance with anisotropic correlation lengths

Figure 32 illustrates one realization of the permeability field for the best estimate permeability as well as best estimate variance. The H.C.L is ten times longer than the V.C.L (k = 269mD, sill = 0.526, H.C.L = 27m and V.C.L = 2.7m). Long high permeable pathways in horizontal direction are observed in this case due to large anisotropy in correlation lengths (Figure 32). The high permeable pathways are having a significantly larger effect on the distribution of $scCO_2$ than the buoyancy effect, resulting in a increased horizontal migration of $scCO_2$ though the high permeable pathways (Figure 33).The buoyancy effect is significantly larger after a redistribution period and the high permeable pathways are still having a larger impact on the distribution of the scCO2 plume (Figure 34).

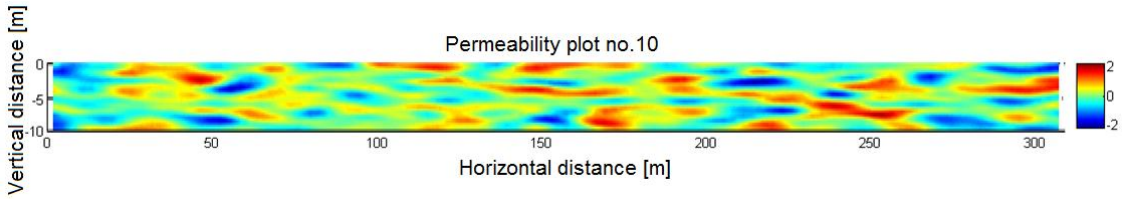

Figure 32 Example permeability field for high permeability, best estimate variance and large anisotropy in correlation lengths (realization B331).

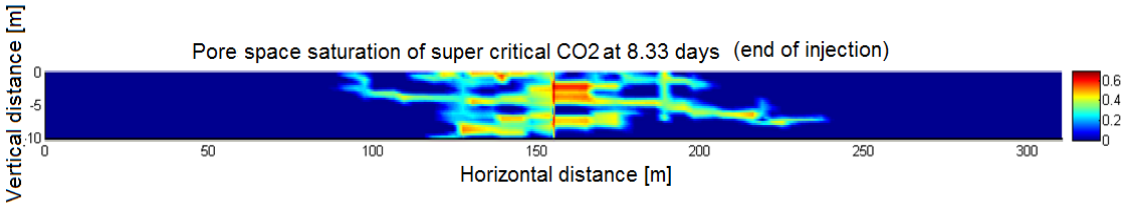

Figure 33 Super critical CO_2 saturation at 8.33 days of injection.

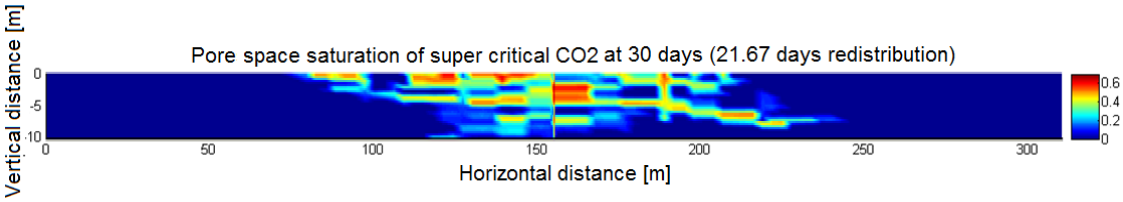

Figure 34 Super critical CO_2 saturation at 30 days including 8.33 days injection.

4. ANALYSIS OF RESULTS FROM MULTIPLE REALIZATIONS AND DISCUSSION

The following figures in chapter 4.1 - 4.4 contain data representing the median values of 40 randomized realizations (solid data points). Data points at zero horizontal correlation length (non-solid data points) represent the result of a homogeneous case.

4.1 DISSOLVED MASS

The combined (median) results of the multiple realizations for total amount of dissolved CO_2 in the aqueous phase are shown in Figure 35 (after 8.3 days of $scCO_2$ injection) and Figure 36 (after 21.7 of days additional redistribution i.e. 30 days after start of injection). Comparing Figure 35 with Figure 36 gives a possibility to observe the dissolved mass fraction after the injection period of 8.33 days with the dissolved mass fraction after a redistribution period of 21.67days. As the results show in Figure 35, a generally smaller mass fraction dissolved CO_2 occurs right after the injection phase compared to after the redistribution period shown in Figure 36, which is expected due to the $scCO_2$ migration during the redistribution phase. Note that the same overall trends can be observed in both figures even though Figure 36 indicates an overall higher mass of CO_2 dissolving in the aqueous phase. That is; the median results of the 40 realizations created for each horizontal correlation length distance show a slight variation in trends but still indicate an overall increased amount dissolved CO_2 to the aqueous phase as the horizontal correlation length, permeability as well as the degree of heterogeneity becomes higher.

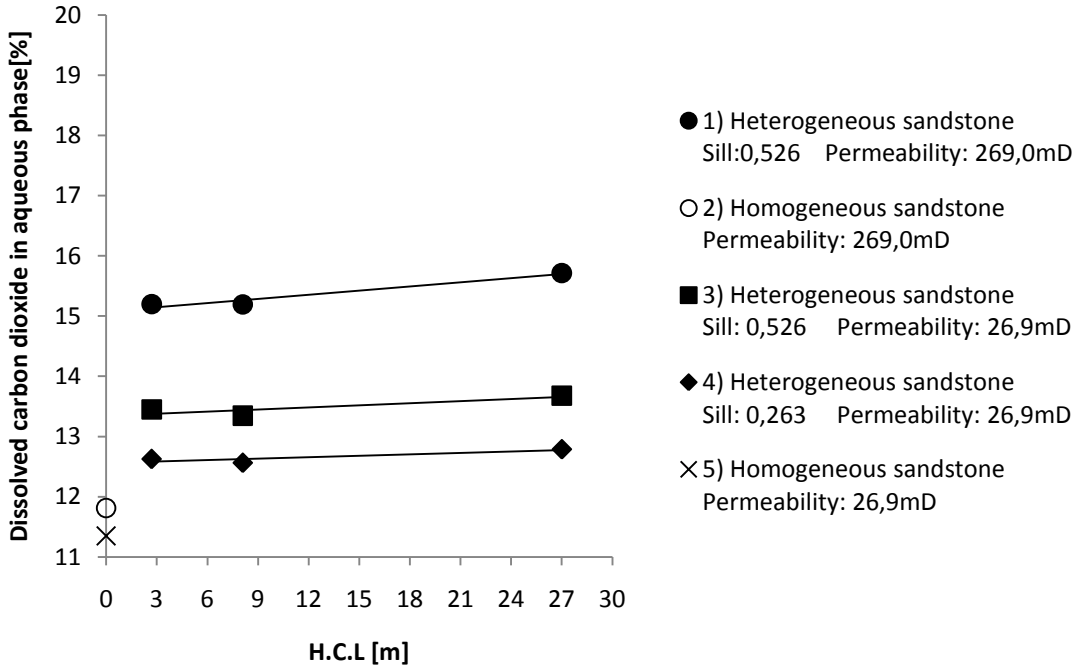

Figure 35 8.33 days. The median amount dissolved super critical carbon dioxide mass fraction within section A (see Chapter 2.3 for more information about section A).

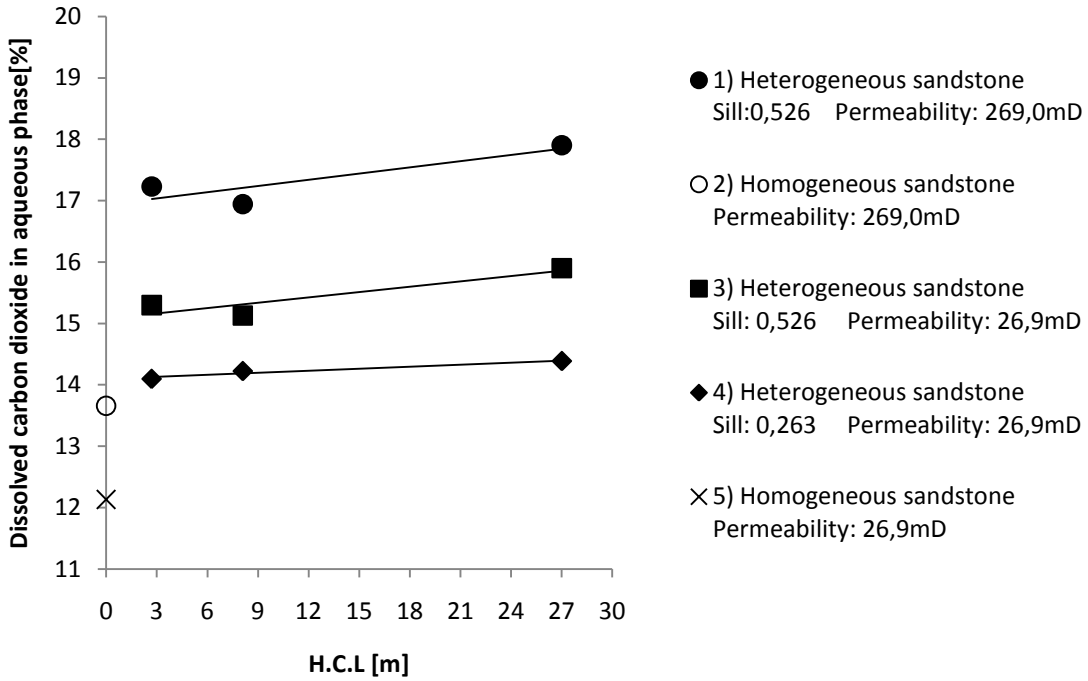

Figure 36 30 days. The median amount dissolved super critical carbon dioxide mass fraction within section A (see Chapter 2.3 for more information about section A).

In Figure 36, the overall trend suggests that a higher degree of heterogeneity (sill) result in a higher amount of dissolved CO_2. As for the horizontal correlation length the trend is not as convincing when comparing horizontal correlation length 2.7m with 8.1m which gives mixed signals. The limited amount of realizations, 40, on the other hand gives room for some uncertainty. Remarkable about the data for horizontal correlation length is that the results for 27 meter indicate on a much higher amount of dissolved CO_2 to the aqueous phase and therefore the overall results suggests that the amount of dissolved CO_2 to the aqueous phase has a significant but weak positive correlation to the horizontal correlation length. In other words, the results suggest that the amount of dissolved CO_2 is affected by the sill as well as the horizontal correlation length. The results also show that the degree of dissolved CO_2 in the aqueous phase is more affected by variance in permeability than by the horizontal correlation length, even though both have a significant impact on the amount of dissolved CO_2.

The results indicate that an increased permeability creates a shift in the dissolved mass fraction of CO_2 and that amount of dissolved CO_2 still has the same positive correlation to the horizontal correlation length and sill even though the permeability is varied (Figure 36).

It is questionable if the relation between horizontal correlation length and dissolved CO_2 is linear or better described with a function of different order but the significantly higher values at horizontal correlation length 27 meter compared to results for shorter lengths indicate a positive correlation between horizontal correlation length and dissolved CO_2.

iTOUGH2 assumes a equilibrium dissolution at the slightest occurrence of $scCO_2$ within a element which is an assumption compromising the results accuracy. Even so, a higher amount of dissolved CO_2 suggests that a larger volume of the aquifer is being used for $scCO_2$ and thus indicating on lower pore space saturation within the affected areas within the aquifer.

The following were the main observations made about CO_2 dissolution in the different cases:

- Cases of heterogeneity have a significantly higher amount dissolved CO_2 in aqueous phase than in there corresponding homogeneous cases.
- Cases of lower variance than the B.E show a lower amount dissolved CO_2
- Cases of higher permeability show higher values for dissolved CO_2.
- Variance and average permeability have a bigger impact on the amount dissolved CO_2 than the H.C.L.
- A higher amount of dissolved CO_2 occurs after redistribution.

4.2 VOLUMETRIC STORAGE

Figure 38 confirms the reasoning that a larger portion of the aquifer contains $scCO_2$ in the presence of heterogeneity. The higher the sill the larger the aquifer volume containing CO_2 becomes. Figure 38 shows that an increased permeability result in a wider migration of $scCO_2$ when comparing the homogeneous case of k=269 with the homogeneous case of k=26.9. Just like the results concerning dissolved mass CO_2 in Figure 36, the results in Figure 38 indicate the same positive correlation to horizontal correlation length, permeability and variance in permeability as discussed in chapter 4.2. Figure 37 compared with Figure 38 show that the same general trends occur at right after the injection phase as well as after redistribution.

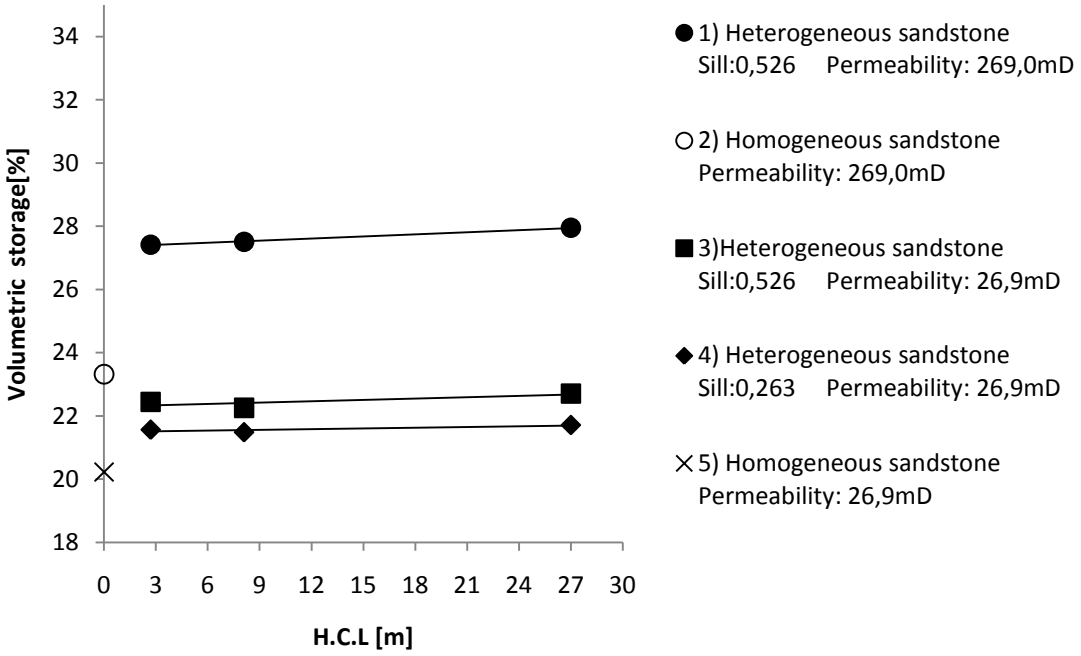

Figure 37 8.33 days. Median percentage simulation blocks containing super critical carbon dioxide in section A (see Chapter 2.3 for more information about section A).

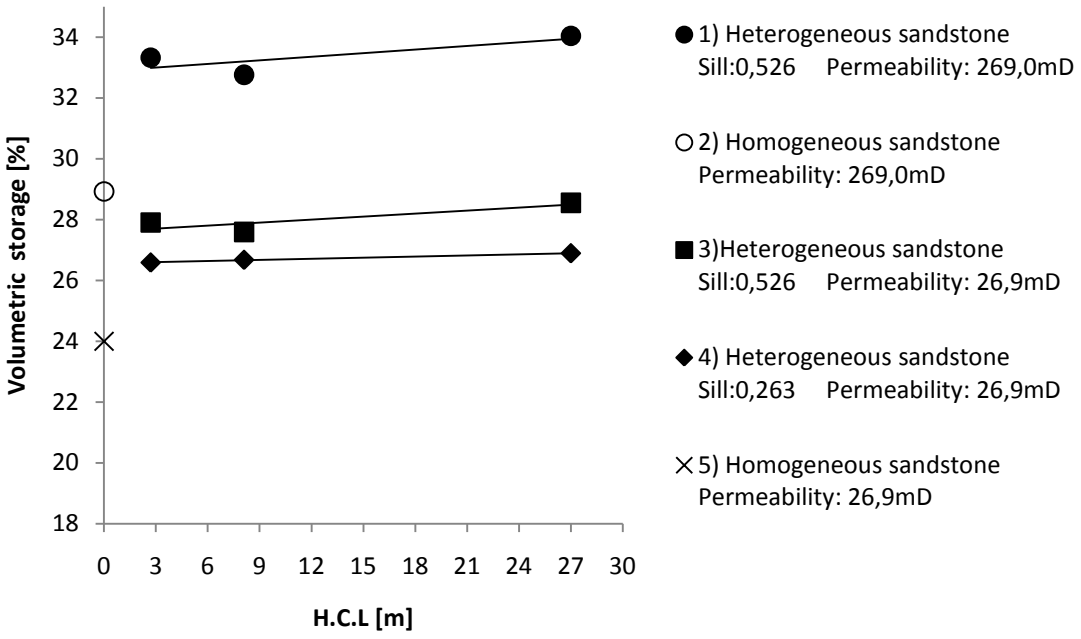

Figure 38 30 days. Median percentage simulation blocks containing super critical carbon dioxide in section A (see chapter 2.3 for more information about section A).

The following were the main observations made about CO_2 volume in the different cases:

- Cases of heterogeneity show that a significantly larger volume of the aquifer has been affected by the CO_2 plume than in corresponding homogeneous cases.
- Cases of lower variance than the B.E show that a significantly larger volume of the aquifer has been affected by the CO_2 plume.
- Cases of higher permeability show that a significantly larger volume of the aquifer has been affected by the CO_2 plume.
- Variance and average permeability have a larger impact on the spread of the plume than the H.C.L.
- A larger volume of the aquifer has been affected after redistribution.

4.3 STORAGE EFFICIENCY

Even though the results so far suggest an increased volume is higher for cases of higher average permeability, variance in permeability and horizontal correlation length, it does not tell us how efficient the storage space usage is. Therefore a specific measure was applied in order to make a better observation. In this thesis the measurement used to describe the efficiency are introduced the ratio of total injected CO_2 mass and volume of formation pore space associated with the maximum spread of CO_2, see

Table ***2***. The measurement indicates a less effective usage of the aquifer's storage space for lower values.

First of all, a comparison between Figure 39 and Figure 40 shows that the efficiency is much higher at the end of the injection phase than after redistribution. By the end of the redistribution phase the efficiency has dropped markedly for all simulated cases (Figure 40). The same overall trend can still be observed except in the homogeneous case of k=269 sill=0.526 where the efficiency is reduced much more after a redistribution period (Figure 40).

The simulations of Heletz low permeability, k=26.9, together with its high degree of heterogeneity, sill=0.526, indicate less storage efficiency compared to the homogeneous base case of Heletz, k=26.6. Simulations with only half the degree of heterogeneity, sill=0.263 gives a larger storage efficiency value indicating that the heterogeneity has a negative correlation to storage efficiency (Figure 40).

Not as obvious is the correlation between storage efficiency and horizontal correlation length. Some irregular tendencies occur at horizontal correlation length 8,1meter but the overall trend is strong enough for the horizontal correlation length at 27meter to suggest that horizontal correlation length has a negative correlation to storage efficiency (Figure 40).

Interestingly enough the case of a higher permeability in Figure 40, k=269 sill=0.526, has an even lower storage efficiency compared to the heterogenic cases, k=26.9 sill=0.263 and k=26.9 sill=0.526.

The results shown in Figure 40 also indicate that the investigated heterogeneity in hydraulic conductivity of Heletz storage material, in extreme cases such as k=26.9, sill=0.526 and a horizontal correlation length of 27 meter, can be almost equally storage efficient as a ten times more permeable homogeneous aquifer. This is interesting from an economic point of view since injections into materials of low permeability generally are more energy demanding due to the demand of higher injection pressure. Perfectly homogeneous sandstone does not exist in nature but the results point out the fact that a low permeable storage material with a high degree of heterogeneity does not necessarily have to be better suited for storage when taking economic aspects into account. If given the alternative to use a storage site with higher permeability and less heterogeneous characteristics one should consider such an alternative as well. Even so the majority of

the results indicate that a low average permeability, low variance in permeability and short horizontal correlation length increases the chances for a more efficient usage of the storage site capacity.

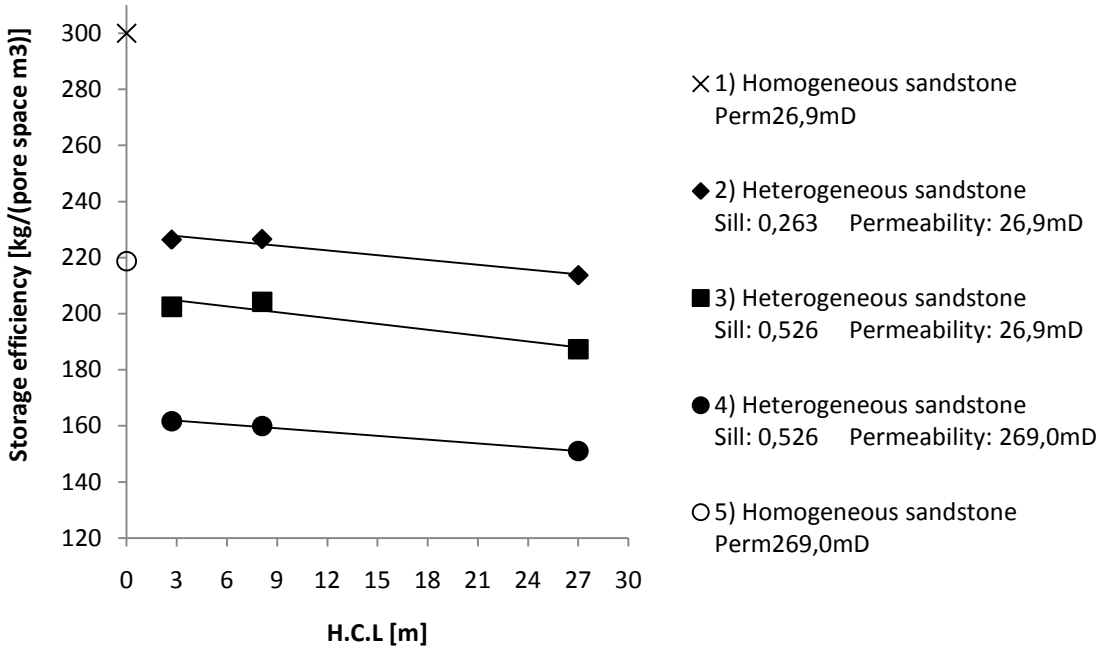

Figure 39 8.33 days. Median storage efficiency of $scCO_2$.

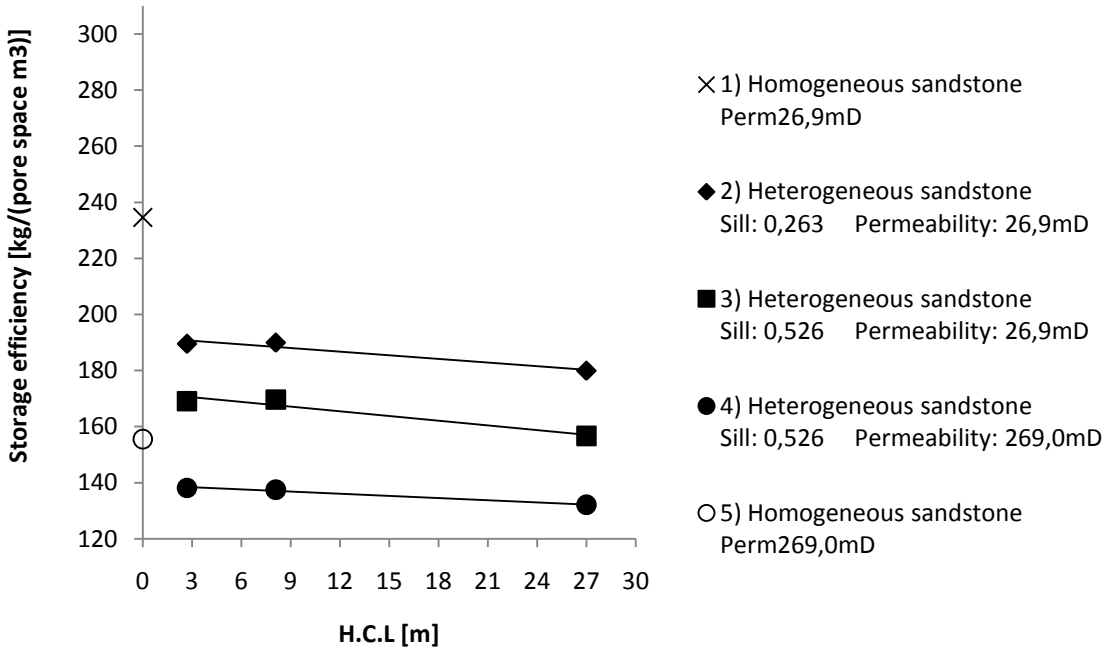

Figure 40 30 days. Median storage efficiency of $scCO_2$.

The following were the main observations made about storage efficiency in the different cases:

- Cases of heterogeneity show that a significantly larger volume of the aquifer has been affected by the CO_2 plume than in corresponding homogeneous cases.
- Cases of lower variance than the B.E show that a significantly larger volume of the aquifer has been affected by the CO_2 plume.
- Cases of higher permeability show that a significantly larger volume of the aquifer has been affected by the CO_2 plume.
- Variance and average permeability have a larger impact on the spread of the plume than the H.C.L.
- The storage efficiency becomes even lower after redistribution.

4.4 MAXIMUM MIGRATION DISTANCE

Comparing Figure 41 with Figure 42 shows that the same maximum migration distance has the same trends before and after the used redistribution period. The efficiency measure is based on only two variables which are the migration distance on each side of the injection well and are therefore strongly correlated with the results concerning storage efficiency. Even so, looking at the maximum migration distance shows us the underlying tendencies causing lower storage efficiency. Figure 42 has an inverse look compared to Figure 40 due to negative correlation between the maximum migration distance and storage efficiency. Therefore, the results show that a higher average permeability, variance in permeability and longer horizontal correlation length increases the maximum migration distance. Furthermore, changes in permeability indicate that a ten times higher permeability, from k=26.9 to k=269, creates a large shift of the maximum migration distance.

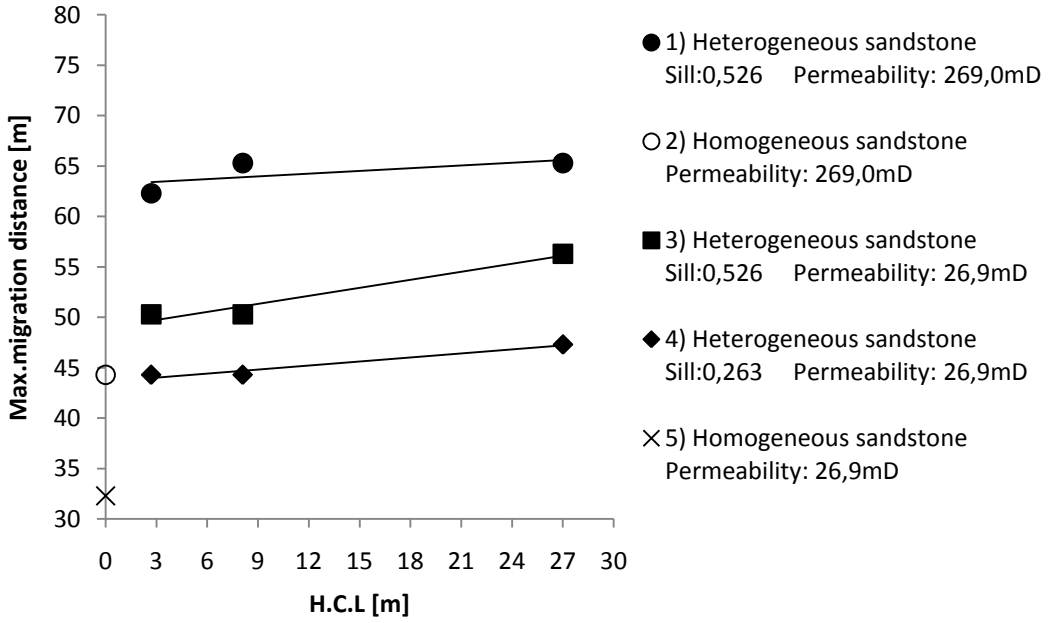

Figure 41 8.33 days. Median maximum migration distance of $scCO_2$

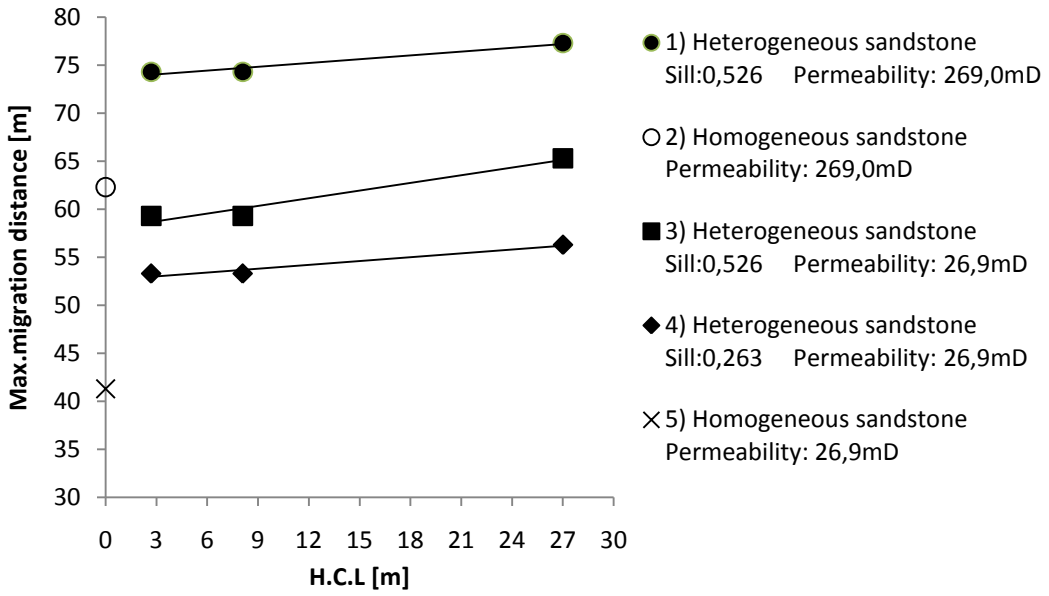

Figure 42 30 days. Median maximum migration distance of $scCO_2$

The following were the main observations made about maximum migration distance (M.M.D) in the different cases:

- Cases of heterogeneity have longer (M.M.D) than the corresponding homogeneous cases.
- Cases of lower variance than the B.E have shorter M.M.D.
- Cases of higher permeability have a significantly longer M.M.D.
- Variance and average permeability have a larger impact on the M.M.D.
- M.M.D increases during redistribution.

4.5 SEMIVARIOGRAM

The experimental model shown in the log-semivariogram, Figure 12, was fitted by honoring lag pairs equal and shorter than 3.7 meter. The amount of lag pairs steadily decreased and the combined core samples of well H13, H18 and H38 sometimes contributed with an unequal amount of lag pairs. At distance 3.7 meter the semivariogram stabilized at the same time as the lag pairs from each core sample are somewhat equal to the amount. Looking further than 3.7 meter the semivariogram became dependent on a smaller amount of lag pairs at the same time as individual core samples contributed with an uneven amount of pairs. As a result to that the log-semivariogram started to oscillate heavily and therefore shorter lag pairs were honored by using the parameters listed in Table 4. The outcome is shown in Figure 12.

When examining the permeability data through histograms, the data proved to be of a log-normal rather than a normal distribution. Also, a better fit of the experimental model was made when performing a log-transformation of the permeability data which is the

reason for determining the log-semivariogram shown in Figure 10. The indicated log-normal distribution of the permeability data can be observed in Figure 9.

4.6 ERRORS

Maximum pressure at the end of the simulations reached values around 41 000 kPa in the cases of low permeability around the injection well. The naturally occurring pressure at the Heletz aquifer is estimated to roughly 14 700 kPa. It is expected that if an injection were to be made, in reality, with such a high pressure difference, the cap rock might be damaged. A slower injection rate together with a longer injection period could be simulated in order to correct the pressure build up. This is instead ignored with the motivation that the governing equations together with the boundaries used do not take the cap rock into account and therefore the high pressure does not affect the results in a negative way and still describes the heterogeneity's significance in a correct way.

5 CONCLUSION

The results show that saline aquifers with low permeability, such as the target layer of Heletz storage site, reach higher storage efficiency for scenarios with a smaller variance in permeability (sill) and a shorter horizontal correlation length. For the same rate of injection, a higher permeability produces a larger horizontal migration of CO_2, which in its turn decreases the storage efficiency in comparison to the case of less permeable storage formation. Therefore, this study suggests that the storage efficiency of deep saline aquifers decreases for higher values of average permeability, variance in permeability and horizontal correlation length within the investigated intervals.

The reason for the decreased storage efficiency, as a result of a smaller variance in permeability, is observed in the high and low permeable pathways that form when variance and horizontal correlation length are high. The high permeable areas enable the $scCO_2$ to migrate further at the same time as extremely low permeable areas force the $scCO_2$ to bypass. A horizontal correlation length elongates the high permeable areas creating pathways of preferential flow that decrease the storage efficiency even further.

It can be concluded that the average permeability governs the buoyancy flow and subsequent preferential flow along the formation ceiling, while the heterogeneity in the permeability field governs preferential flow along high-permeability pathways. Comparing how these processes affect the storage efficiency, the results further indicate that the heterogeneous Heletz aquifer, given a horizontal correlation length ten times larger than the vertical correlation length, has similar storage efficiency to that of a ten times more permeable homogeneous formation.

6 REFERENCES

Barnes R. J. (1991). Teacher's Aide: The Variogram Sill and the Sample Variance, *Mathematical Geology*, Vol.23, p.673-678.

Brooks R. H. and Corey A. T. (1964). *Hydraulic properties of porous media.* Hydrology Papers, vol 3. Colorado State University. Fort Collins Colorado.

CO_2MUSTANG. (2011-03-13). http://www.co2mustang.eu/Heletz.aspx.

Doughty C. and Pruess K. (2004). Modeling Supercritical Carbon Dioxide Injection in Heterogeneous Porous Media. *Vadose Zone Journal*, Vol.3, p.837–847.

Finsterle S. and Kowalsky M. B. (2007). *iTOUGH2-GSLIB User's Guide*. Earth Sciences Division, Lawrence Berkeley National Laboratory, University of California, Berkeley.

Flett M., Gurton R. and Weir G. (2007). Heterogeneous saline formations for carbon dioxide disposal: Impact of varying heterogeneity on containment and trapping. *Journal of Petroleum Science and Engineering, Vol.57, p106-118.*

Fagerlund F., Niemi A., Bensabat J., Rasmusson M., Rasmusson K., Tian L., Shtivelman V. and Licha T. (2010). *Design and Analysis of Field Experiments for the Investigation of In-Situ CO2 Trapping, Abstract H13C-0981*, 2010 Fall Meeting, AGU, San Francisco, Calif., 13-17 Dec.

Fagerlund F., Niemi A. and Odén M. (2006). Comparison of relative permeability–fluid saturation–capillary pressure relations in the modeling of non-aqueous phase liquid infiltration in variably saturated, layered media. *Advances in Water Resources*, Vol.29, p.1705-1730.

Hovorka S. D., Doughty C. and Holtz M. H. (2004). *Testing Efficiency of stroage in the subsurface: Frio brine pilot Experiment.* Gulf Coast Carbon Center, Bureau of Economic Geology, Jackson School of Geosciences. The University of Texas at Austin. Lawrence Berkeley National Laboratory.

IPPC (2005). *IPCC Special Report on Carbon dioxide Capture and Storage*. International Panel on Climate Change.

IPPC (2007). *Climate Change 2007: Synthesis Report*. International Panel on Climate Change.

Leverett M. C. (1941). Capillary behavior in porous solids. *AIME Transactions*, Vol.142, p.152–169.

de Marsily G. (1986). *Quantitative Hydrogeology, Groundwater Hydrology for Engineers*. Academic Press Inc. Orlando, FL, USA.

Niemi A. (1994). *Modeling flow in fractured medium, Uncertainty analysis with stochastic continuum approach.* Technical Research of Finland. Dissertation Thesis.

Pruess K. (2005). *ECO2N: A TOUGH2 Fluid Property Module for Mixtures of Water, NaCl, and CO_2.* Earth Sciences Division, Lawrence Berkeley National Laboratory, University of California, Berkeley.

Pruess K., Oldenburg C. and Moridis G. (1999). *TOUGH2 USER'S GUIDE, VERSION 2.0*. Earth Sciences Division, Lawrence Berkeley National Laboratory, University of California, Berkeley.

UNCERT. (2011-03-13). http://www.uncert.com/tutor/.

UNFCC. (2011-03-13). http://unfccc.int/kyoto_protocol/items/2830.php

APPENDIX 1

Input file used to specify material properties in iTOUGH2

```
ROCKS----1----*----2----*----3----*----4----*----5----*----6----*----7----*----8
SANST     2     2600.       .172 269.0e-15 269.0e-15 269.0e-15      2.51       920.
   4.5e-10
   10             0.3       0.09
   10           0.762    11.83E3     1.0E10     1.0E-3
WELLL     2     2600.       .999 269.0e-15 269.0e-15 269.0e-15      2.51       920.
   4.5e-10
   10             0.3       0.09
   10           0.762     1.0E-3     1.0E10     1.0E-3
FAKEE     2     2600.       .172 269.0e-15 269.0e-15 269.0e-15      2.51       920.
   4.5e-10
   10             0.3       0.09
   10           0.762    11.83E3     1.0E10     1.0E-3

MULTI----1----*----2----*----3----*----4----*----5----*----6----*----7----*----8
    3    3    3    6
SELEC....2....3....4....5....6....7....8....9...10...11...12...13...14...15...16
    1                                        0    0    0    0    0    0    0    0
        .8         .8
SOLVR----1----*----2----*----3----*----4----*----5----*----6----*----7----*----8
5  Z1   O0    8.0e-1    1.0e-7
START----1----*----2----*----3----*----4----*----5----*----6----*----7----*----8
----*----1 MOP: 123456789*123456789*1234 ---*----5----*----6----*----7----*----8
PARAM----1----*----2----*----3----*----4----*----5----*----6----*----7----*----8
   19999    99991000 00000200  4    0  7
            2.592e6       -1.                           9.81
    1.E-1
    1.E-05     1.E00                                 1.E-8
             1.47e7              .04988                                    67.
MOMOP----1----*----2----*----3----*----4----*----5----*----6----*----7----*----8
    1
```